ACS OMEGA

http://pubs.acs.org/journal/acsodf

Article

Deciphering the Proteomic Landscape of *Mycobacterium tuberculosis* in Response to Acid and Oxidative Stresses

Eira Choudhary, Rishabh Sharma, Pramila Pal, and Nisheeth Agarwal*

Cite This: *ACS Omega* 2022, 7, 26749−26766

Read Online

ACCESS | Metrics & More | Article Recommendations | Supporting Information

ABSTRACT: The fundamental to the pathogenicity of *Mycobacterium tuberculosis* (Mtb) is the modulation in the control mechanisms that play a role in sensing and counteracting the microbicidal milieu encompassing various cellular stresses inside the human host. To understand such changes, we measured the cellular proteome of Mtb subjected to different stresses using a quantitative proteomics approach. We identified defined sets of Mtb proteins that are modulated in response to acid and a sublethal dose of diamide and H_2O_2 treatments. Notably, proteins involved in metabolic, catalytic, and binding functions are primarily affected under these stresses. Moreover, our analysis led to the observations that during acidic stress Mtb enters into energy-saving mode simultaneously modulating the acid tolerance system, whereas under diamide and H_2O_2 stresses, there were prominent changes in the biosynthesis and homeostasis pathways, primarily modifying the resistance mechanism in diamide-treated bacteria while causing metabolic arrest in H_2O_2-treated bacilli. Overall, we delineated the adaptive mechanisms that Mtb may utilize under physiological stresses and possible overlap between the responses to these stress conditions. In addition to offering important protein signatures that can be exploited for future mechanistic studies, our study highlights the importance of proteomics in understanding complex adjustments made by the human pathogen during infection.

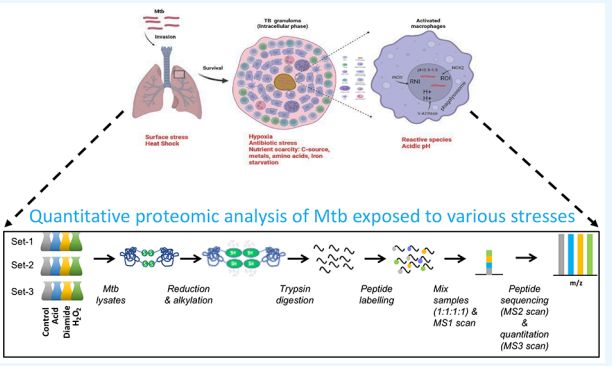

INTRODUCTION

Even though tuberculosis (TB) is curable and preventable, it remains one of the leading causes of mortality from a single infectious agent.[1] Because of COVID-19 pandemic, global TB targets have experienced a major setback causing not only a huge drop in the diagnosis, reporting, and treatment of new cases worldwide, but also triggering an ominous rise in total deaths. With 1.3 million TB deaths, as compared to 1.2 million in 2019, in HIV negative individuals, and almost 15% reduction in the treatment for drug-resistant TB between 2019 and 2020, there is a rising demand for reversing these impacts and to work toward resolving these shortfalls.[1]

The ability of several intracellular pathogens like *Mycobacterium*, *Salmonella*, *Shigella,* and so on to reside and persist inside phagocytotic cells largely depends on their mechanism to neutralize host immune responses, reprogramming of the host's as well as pathogen's metabolism, and resistance against the hostile environment of activated macrophages and related endocytic compartments.[2,3] The adaptation of *Mycobacterium tuberculosis* (Mtb) to extracellular conditions by surviving and replicating inside the microbicidal milieu of macrophages is in part responsible for its success as a deadly pathogen. Moreover, there is compelling evidence of the presence of the bug inside the heterogeneous lesions during infection, thereby pointing to its ability to endure the plethora of host microenvironments.[4] Once phagocytosed by the resting macrophages, Mtb is exposed to reactive oxygen intermediates generated by host phagocyte oxidase (NOX2).[5] After activation with IFN-γ, Mtb is inside the acidic environment of phagolysosomes and encounters reactive nitrogen intermediates from inducible nitric oxide synthase.[6] This implies the highly potent environment of host cells to resist the infection. Nevertheless, mycobacterial pathogens have evolved a plethora of mechanisms to defuse host-inflicted stresses such as oxidative and nitrosative stress and low pH in combination with other stressors like nutrient deprivation, metal toxicity, and iron deficiency. Several studies using genomics and transcriptomics have unearthed the molecular factors governing the adaptation of Mtb withstanding nitro-oxidative stresses and acidic pH.[7,8] It is shown that Mtb possesses the detoxification system, including antioxidant enzymes superoxide dismutase (SodA and SodC),[9] catalase (KatG),[10] alkyl hydroperoxide reductase (AhpC),[11] and a redox buffering system-mycothiol[12]

Received: May 18, 2022
Accepted: July 5, 2022
Published: July 18, 2022

https://doi.org/10.1021/acsomega.2c03092
ACS Omega 2022, 7, 26749−26766

among others. The cell wall components like peptidoglycan and cell wall lipid lipoarabinomannan have been shown to participate in resisting the acidic concentration of the phagolysosomal compartment.[13] Moreover, the role of OmpA (outer membrane protein A),[14] Mg^{2+} transporter MgtC,[15] and membrane-associated serine protease *Rv3671c*[16] is well documented for the maintenance of cell wall integrity during acidic stress. However, these reports provide evidence that resistance and adaptation to these stresses are well placed in Mtb facilitating the in vivo growth and persistence of the pathogen.

While these studies revealed an array of genes that are regulated at transcript levels, changes in the expression of mycobacterial proteins under different experimental conditions have also been studied. Proteome analysis of Mtb during normoxia,[17] dormancy,[18] reactivation,[19] and nitrosative stress[20] has provided insights into the molecular mechanisms that are regulated at different stages of the pathogen's life cycle inside the host. However, we are yet to recognize the proteomic response of Mtb under low-pH and oxidative conditions. To this fact, understanding the global proteome of mycobacterium under multiple stress conditions will serve as a functional complement to data available from other omics approaches, and a more holistic view of the molecular network of stressed mycobacterium to a combination of stresses could be generated.

With an aim to understand how bacteria adapt to stresses, herein we performed the global proteome profiling of virulent Mtb H_{37}Rv upon exposure to acidic and oxidative stresses during in vitro growth. Based on information from previous studies, we exposed the bacterial culture to a sublethal dose of diamide as a thiol oxidizer, hydrogen peroxide as an inducer of peroxide stress[21,22] and growth medium with pH 5.5 conferring acidic stress.[23] We employed iTRAQ (isobaric tags for relative and absolute quantification) coupled with liquid chromatography mass spectrometry (LC−MS) to identify differentially expressed proteins (DEPs) in the stressed Mtb H_{37}Rv. Analyses of proteomic data using bioinformatic tools reveal the rewiring in Mtb molecular networks during oxidative and acidic stresses causing perturbations in metabolic and biosynthesis pathways, which together suggest the intriguing function of cellular proteins in regulating mycobacterium adaptation to host cell stressors.

EXPERIMENTAL PROCEDURES

Bacterial Strains, Media, and Growth Conditions. All experiments are performed with the *Mycobacterium tuberculosis* H_{37}Rv strain. For liquid culture, Mtb was grown with gentle agitation at 37 °C in Middlebrook 7H9 broth (MB7H9) (Difco) supplemented with sterile 10% Oleic acid-albumin-dextrose-saline (OADS) enrichment, 0.5% glycerol, and 0.05% tyloxapol. For the CFU experiment, Middlebrook 7H11 (MB7H11) (Difco) was supplemented with 10% OADS enrichment and 0.5% glycerol.

In Vitro Growth under Different Stress Conditions. Different in vitro stress conditions were standardized based on the growth analysis of Mtb in the presence of stress agents. The wild-type H_{37}Rv was harvested at 0.7 OD_{600} and washed twice with 1X PBS, before treating with different stressors. For acidic stress, washed bacterial cells were suspended in MB7H9 medium set in various pH ranges viz. pH 7.0, pH 6.5, pH 5.5, and pH 4.5 and incubated for 5 days at 150 rpm and 37 °C. For thiol-mediated oxidative stress, bacterial cells were suspended in 7.5 mL of MB7H9 medium, and each tube was treated with different diamide concentrations viz. 0.5, 1, 5, 10, and 20 mM, whereas in the case of H_2O_2-mediated oxidative stress various concentrations of H_2O_2 viz. 0.05, 0.5, 5, 10, and 50 mM were added. The untreated (UT) culture was taken as a reference control in both stresses. All the cultures were incubated at 150 rpm and 37 °C for different time intervals, that is, 0, 4, 16, 24, 48, and 120 h. In vitro growth analysis was performed by measuring optical density (OD) at each time point.

Whole Cell Lysate (WCL) Preparation. The WCL of Mtb was prepared from three independent replicates of control and stressed samples as follows: post-16 h of stress treatment, 40 mL of Mtb culture at an OD_{600} of ∼0.70 was pelleted down and washed three times with 1X PBS. The pellet was suspended in lysis buffer containing 1X PBS and a protease inhibitor cocktail (Sigma). Furthermore, Mtb cells were lysed by bead-beating using 0.1 mm zirconia beads, and the cell lysate was centrifuged at 12000 rpm. The supernatant was collected and filtered twice with a 0.2 μm filter. For total protein quantification, BCA assay was performed (Thermo Fisher Scientific, Waltham, MA) as per the manufacturer's instructions. The WCLs from all treated and untreated samples were also run on 12% SDS-PAGE gel, for quality check.

Experimental Design and Statistical Rationale: iTRAQ-Based Mass Spectrometry. The iTRAQ study was typically performed as described earlier in ref 24. The brief protocol for proteome analysis is as follows: 25 μg of WCL proteins from three independent sets each of control-pH 7.0, UT, and acidic stress (pH 5.5) and oxidative stress (5 mM of diamide and H_2O_2) treated samples were cleaned by acetone precipitation and resuspended in 20 μL of iTRAQ Dissolution Buffer. Subsequently, samples were denatured by adding 1 μL of 2% SDS and 5 mM TCEP (Tris-(2-carboxyethyl) phosphine) and were incubated for 1 h at 60 °C. Furthermore, the denatured and reduced proteins from each sample were treated with cysteine blocking reagent (8.4 mM of iodoacetamide) and incubated in the dark for 30 min at room temperature. Afterward, each of the above protein samples was digested by 1 μg of trypsin per 25 μg of proteins in 1:25 ratio and incubated overnight at 37 °C for efficient digestion. Peptides from three biological repeats each of control and stressed samples from acid, diamide, and H_2O_2 stresses were labeled with 4-plex iTRAQ labeling reagents, in proportion to the standard Applied Biosystems Kit protocol. In biological replicate sets 1 and 3, we labeled control samples with iTRAQ labeling dye 114, while stress-treated samples viz. acid, diamide, and H_2O_2 were labeled with 115, 116, and 117 dyes, respectively, while in set 2 we applied dye switching and labeled the control with 117 and stress samples with iTRAQ dyes 116 (acidic stress), 115 (diamide stress), and 114 (H_2O_2 stress). Labeled peptides of control and stress samples from respective treatments were mixed followed by vacuum drying. The labeled peptide mixture was fractionated by 5 μm particle size of the cation exchange (SCX) column (2.1× 150 mm) using a PerkinElmer Flexar HPLC system. After SCX fractionation, eluted fractions were vacuum-dried and reconstituted for the LC−MS/MS separation. Furthermore, for the second-dimensional separation, spotting of peptides was performed on the Chromolith Caprod RP-18e HR capillary column (150 × 0.1 mm; Merck Millipore). For the identification of proteins, raw files were searched using the Paragon algorithm mediated search mode in ProteinPilot software version 4.0 (AB SCIEX)[25] against the Uniprot *Mycobacterium tuberculosis* proteome database. A decoy database search strategy was used to estimate the false discovery rate (FDR). The proteomics data have been deposited with PRIDE with the database identifier PXD015167.

https://doi.org/10.1021/acsomega.2c03092
ACS Omega 2022, 7, 26749−26766

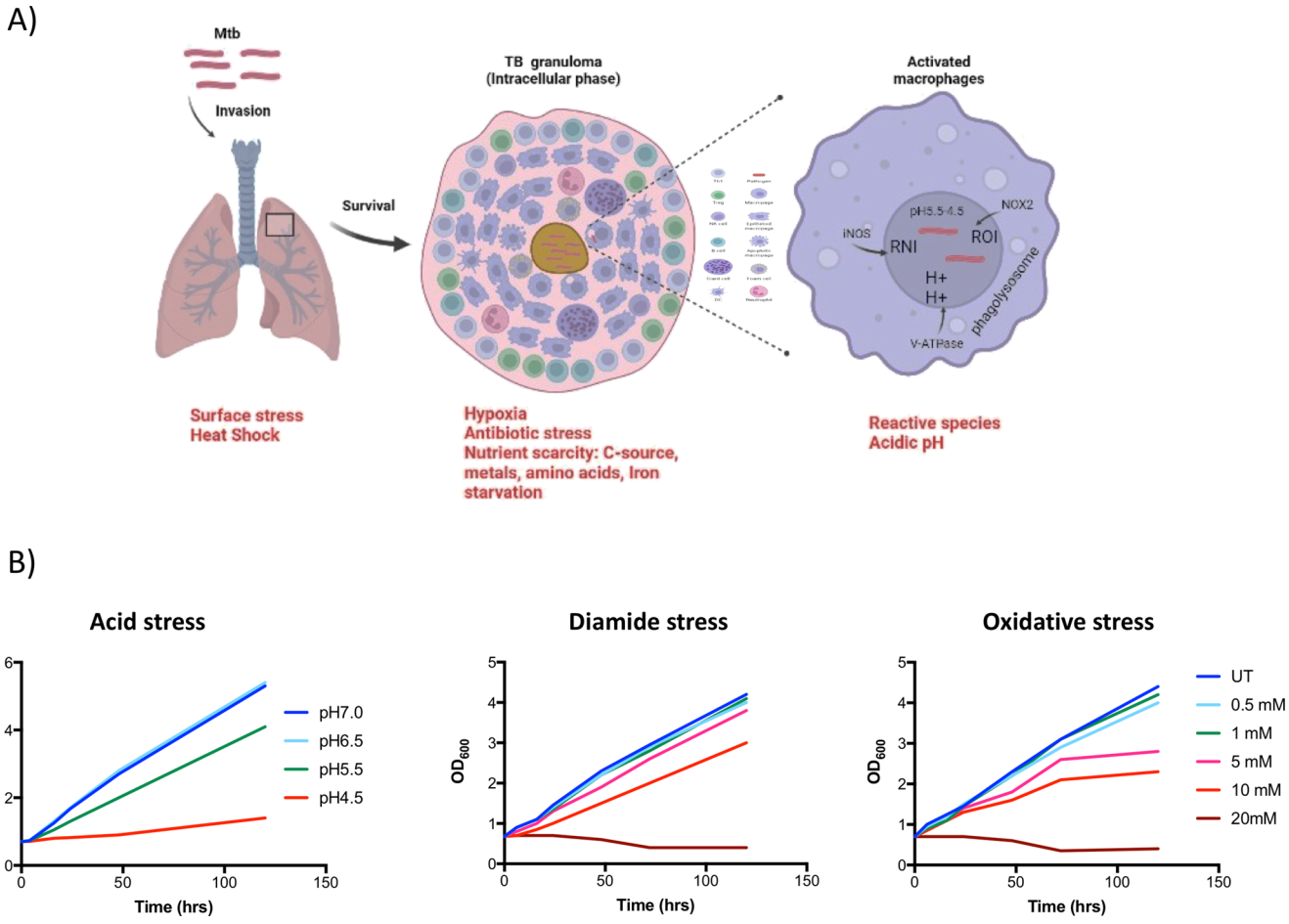

Figure 1. Stress conditions encountered by Mtb inside host and its survival under in vitro stress conditions. (A) Cartoon representing the type of stressors experienced by Mtb inside macrophages during host infection, created with BioRender.com. (B) Growth curve of mycobacteria cultured under different in vitro stress conditions. Mtb was exposed to acidic medium, diamide, and oxidative stress and growth was monitored by OD_{600} estimation at different time points.

The total proteins were quantified using iTRAQ tags. For the relative quantification of peptides in all three sets and samples, only unique peptides were selected of a given protein and those proteins that belong to the same family, or their isoforms were excluded. Moreover, proteins detected with fewer than 1 peptide and those where annotations was performed based on reverse sequencing (RRRRR) were also excluded. The common set of proteins present in all three biological data sets were taken forward to prepare the final data set of individual stresses showcasing fold-change (FC) values of proteins that qualified the above two criteria. The threshold values FC $\geq$ 1.29 and FC $\leq$ 0.77 were applied to the data to identify and classify the over- and under expressed proteins, respectively. We further cross checked the individual values for the consistency in the above-mentioned cutoff across all biological replicates and removed those outlier proteins where the FC value is varying in either of three replicates.

Immunoblotting Analysis. The western analysis was conducted using the same WCL samples that were used for the labeled iTARQ-LC−MS/MS analysis; 20 μg of WCL were dissolved in sample loading buffer containing β-mercaptoethanol and heated at 98 °C for 5 min followed by electrophoresis-based separation on 10% sodium dodecyl sulfate−polyacrylamide gel electrophoresis (SDS-PAGE). The gel was electro-transferred to the nitrocellulose membrane. The blocking was done using 5% nonfat-dried milk (NFDM) containing PBS and 0.1% (v/v) tween 20 (PBST) for 1 h. Afterward, the nitrocellulose membrane was incubated with primary antibodies specific to mycobacterial proteins and overnight at 4 °C. In immunoblotting experiments, primary antibodies viz. anti-FadA and anti-PknB were used at 5000-fold dilution while anti-HtpG was used at 1000-fold dilution, prepared in PBST containing 5% NFDM. After overnight incubation in primary antibodies, membranes were washed three times with PBST buffer followed by 1 h of incubation with 5000-fold diluted horseradish peroxidase-conjugated IgG prepared in PBST containing 3% NFDM. After 1 h of incubation, membranes were washed three times with PBST buffer and blots were developed by SuperSignal West Femto Maximum Sensitivity Substrate (Thermo). Signals were obtained using the ChemiDoc imaging system. Densitometric analysis of the blots was carried out using image processing software (Bio-Rad Laboratories), ImageJ. Relative fold-expression of the proteins was calculated by dividing the band intensities of untreated and treated samples. Statistical analysis of band intensities was performed by Student's t-test.

Gene Ontology (GO) Analysis. The functional enrichment analysis of DEPs identified under different stress conditions was achieved using the ShinyGO (v0.741) application tool (bioinformatics.sdstate.edu/go).[26] The enriched GO biological processes (BPs) and molecular functions (MFs) were labeled for all differential proteins, and only top 30 hallmark pathways were

https://doi.org/10.1021/acsomega.2c03092
ACS Omega 2022, 7, 26749−26766

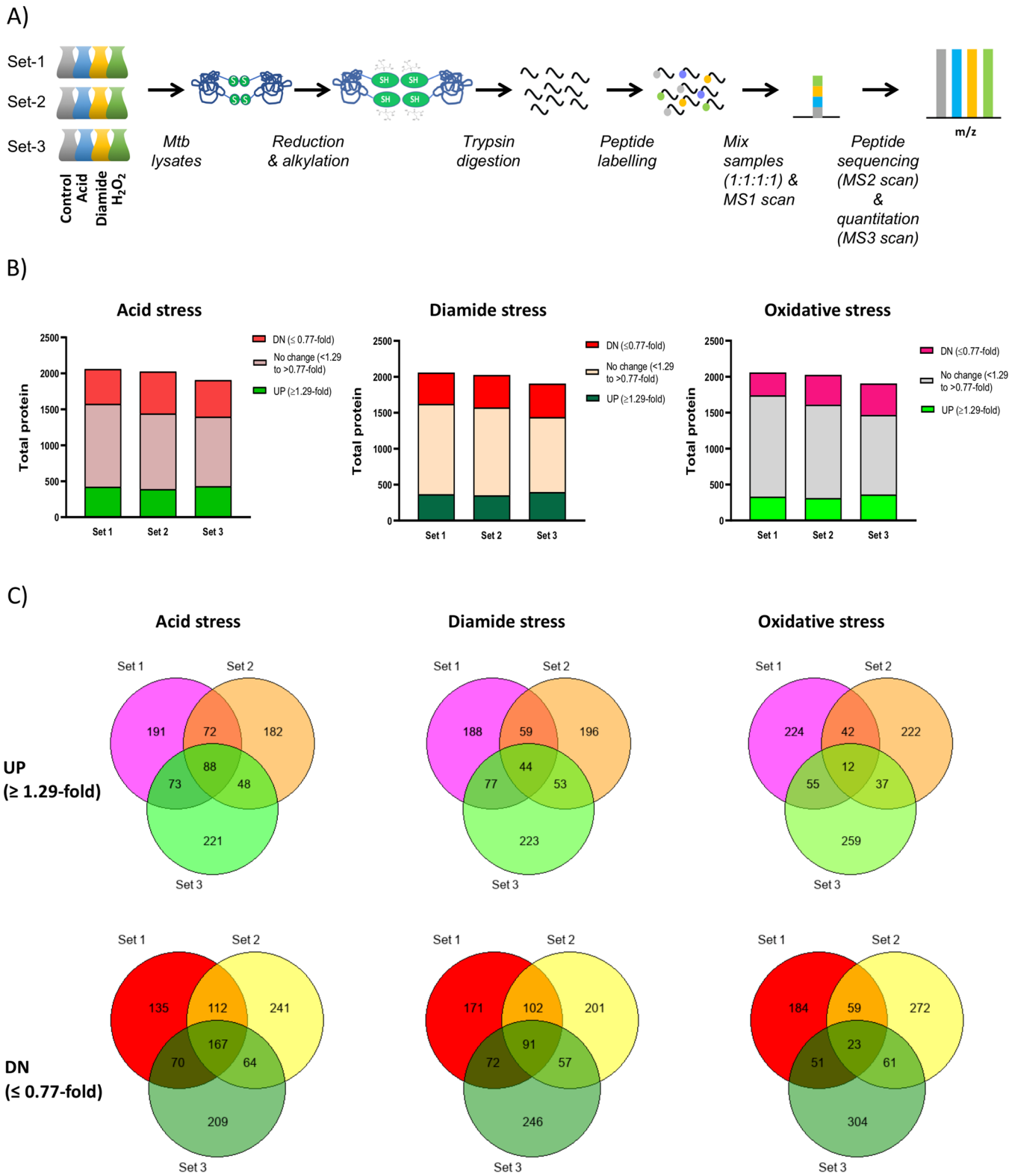

Figure 2. Experimental procedure of proteomic analysis and distribution of total identified proteins. (A) Schematic workflow of iTRAQ mass spectrometry for quantitative proteome analysis of cultured samples. (B) Bar graphs showing upregulated (≥ 1.29-fold) (UP), downregulated (≤ 0.77-fold) (DN), and unaltered (<1.29-fold to >0.77-fold) proteins, identified under different stress conditions and present across three biological replicates. (C) Pie chart distribution of differentially regulated proteins across three biological sets.

selected. An FDR cutoff of <0.05 was used to mark the functional categories as significant.

Protein Interaction and Network Analysis. The DEPs were assessed for protein−protein interaction (PPI) analysis using STRING (11.0) web server.[27,28] The PPI network was performed at a high confidence level of 0.700 allowing all active interaction sources including direct (physical) and indirect (functional) associations. The evidence of these predicted

https://doi.org/10.1021/acsomega.2c03092
ACS Omega 2022, 7, 26749−26766

interactions is presented via genomic context, coexpression, prior knowledge, and high-throughput experiments. The clustering of the association network, based on K-means, was conducted to identify the active functional units present among the target proteins, and only 10 clusters existing within the network were visualized.

RESULTS

Culturing of Mtb H_{37}Rv under Conditions Mimicking the Host Environment. Mtb faces multiple stresses inside host macrophages (Figure 1A). The ability to sense the intracellular hostile conditions and appropriately respond by regulating the expression of a specific set of genes and proteins provides an extended survival benefit to the mycobacterial pathogen.[29] With an objective to identify Mtb proteins that are differentially expressed under a variety of stress conditions, we exposed bacteria to acidic and oxidative (induced by diamide and H_2O_2) stresses that provide the first line of host defense against the infection. For this, we first tested different concentrations of stress agents for a considerable time of exposure to identify the permissible dose with no or minimal effect on the in vitro growth profile of Mtb. In case of acidic stress, cells were grown in 7H9 medium adjusted to pH 7.5, 6.5, 5.5, and 4.5, respectively. Growth was estimated by recording OD_{600} over a period of 120 h. As shown in Figure 1B, Mtb grown in the culture medium at pH 6.5 shows a similar growth pattern to that of culture adjusted to normal pH 7.5. Marginal (16%) reduction in growth is observed upon further reducing the pH of the culture medium to 5.5, whereas substantial (36%) reduction in growth is recorded at pH 4.5, after 16 h of inoculation. In case of culturing at pH 4.5, bacterial growth shows considerable defects of up to 73% until 120 h of treatment; however, at pH 5.5 reasonable growth is seen even after 120 h of growth. Likewise, redox stress was induced by diamide treatment at different concentrations ranging from 0.5 to 20 mM for 120 h. While no discernible deviation in the growth phenotype is observed at 0.5 and 1 mM diamide concentrations in comparison to the untreated control, ∼10% reduction in Mtb growth is seen when bacteria were cultured in the presence of 5 mM diamide. This decline in the in vitro growth is more pronounced in cultures treated with 10 and 20 mM diamide, where up to 22−28 and 36−90% growth arrest is noticed between 16 and 120 h of growth. A similar trend is also noticed when Mtb was grown in culture medium containing different concentrations of hydrogen peroxide (H_2O_2). Shortened (16 h) and prolonged (120 h) exposure to H_2O_2 leads to ∼50 and 90% reduction at the highest (20 mM) concentration of H_2O_2 (Figure 1B). Even 10 mM H_2O_2 also shows lethality ranging from 12 to 50% at these time points. However, bacteria are able to tolerate 5 mM H_2O_2 treatment without showing any substantial cellular death and exhibit only ∼12% reduction until 120 h (Figure 1B). From these results, it is indicative that acidic medium at pH 5.5 and oxidative stress with 5 mM diamide or 5 mM H_2O_2 for 16 h are well tolerated without causing any substantial effect on bacterial proliferation and are therefore ideal for studying the Mtb response to these stresses at the whole cell proteome level.

Global Proteomic Analysis of Mtb in Response to Different Stress Conditions. To gain an insight into the response mechanism of Mtb to a range of conditions mimicking the intracellular stressed host environment, global quantitative proteome analysis was performed. Quantitative proteomics utilizing iTRAQ was carried out to examine the DEPs of Mtb after exposing to multiple in vitro stress conditions, by following a scheme as presented in Figure 2A. Total bacterial lysates were prepared from three different batches (biological repeats), after 16 h of culturing in 7H9 medium at pH 5.5 (acidic stress), in the presence of 5 mM diamide (oxidative stress) or 5 mM H_2O_2 (oxidative stress). To examine any visible change in the expression pattern of proteins across biological replicates, WCLs prepared from different samples were first resolved by 10% SDS-PAGE followed by Coomassie Brilliant Blue staining. From Figure S1, it is evident that the electrophoretic pattern of a variety of proteins ranging from 10 to 120 kDa of both control (C) and the respective treated samples is consistent across all three biological replicates. These samples were subsequently used for identification and quantitation by 4-plex iTRAQ-coupled LC−MS/MS analysis, as described in the Experimental Procedures. Analysis of spectra data identified total 2060 proteins in the replicate-1, 2026 proteins in the replicate-2, and 1907 proteins in the replicate-3.

To identify the stress-responsive proteins, the FC in the expression levels of total proteins obtained from stress-treated samples compared to untreated samples was determined and those exhibiting equal to or less than 0.77-fold change in expression were considered as downregulated, whereas those with equal to or more than 1.29-fold change in expression were considered upregulated. Our results reveal that during acidic stress 424, 390, and 430 proteins are upregulated and 484, 584, and 510 proteins are downregulated in comparison to their levels in the untreated control samples in the three biological replicates, respectively.

During oxidative stress upon diamide treatment, 368, 352, and 397 proteins show upregulation and 436, 451, and 466 proteins show downregulation, whereas in the presence of H_2O_2, expression levels of 333, 313, and 363 proteins are increased and those of 317, 415, and 439 proteins are reduced when compared with untreated control samples, in the three biological sets, respectively (Figure 2B). Taken together, these results highlight that Mtb exhibits modulation of a range of proteins under acid and oxidative stress conditions. Further evaluation of all data sets reveals that 88, 44, and 12 upregulated proteins are consistent across the three biological replicates upon exposure to acid, diamide, and H_2O_2 treatments, respectively. We also observe that 167, 91, and 23 proteins are consistently downregulated in each of the three replicates under the influence of acid, diamide, and H_2O_2 treatments, respectively (Figure 2C and Table S1). Overall, these results signify the physiological impact of stress environments on the global expression pattern of Mtb proteins.

Defining the Proteomic Profile of Mtb Treated with Different Stressors. To gain an insight into the function of regulated proteins, proteome was classified into functional categories as predicted in the Mycobrowser database (https://mycobrowser.epfl.ch/). Of the total 255 proteins showing differential abundances during acidic stress conditions, 28% proteins belong to intermediary metabolism and respiration, 17% to information pathways, 16% to lipid metabolism, and 14% are involved in cell wall and cell processes and remaining 25% are involved in other miscellaneous functions. Likewise, under diamide stress a large proportion of 135 proteins are involved in intermediary metabolism and replication (32%) and lipid metabolism (23%). Furthermore, functional analysis classified the 35 candidate proteins identified under H_2O_2 stress into intermediary metabolism and respiration (34%), conserved hypothetical (23%), information pathways (14%), lipid metabolism (14%), cell wall and cell processes (12%) and

https://doi.org/10.1021/acsomega.2c03092
ACS Omega 2022, 7, 26749−26766

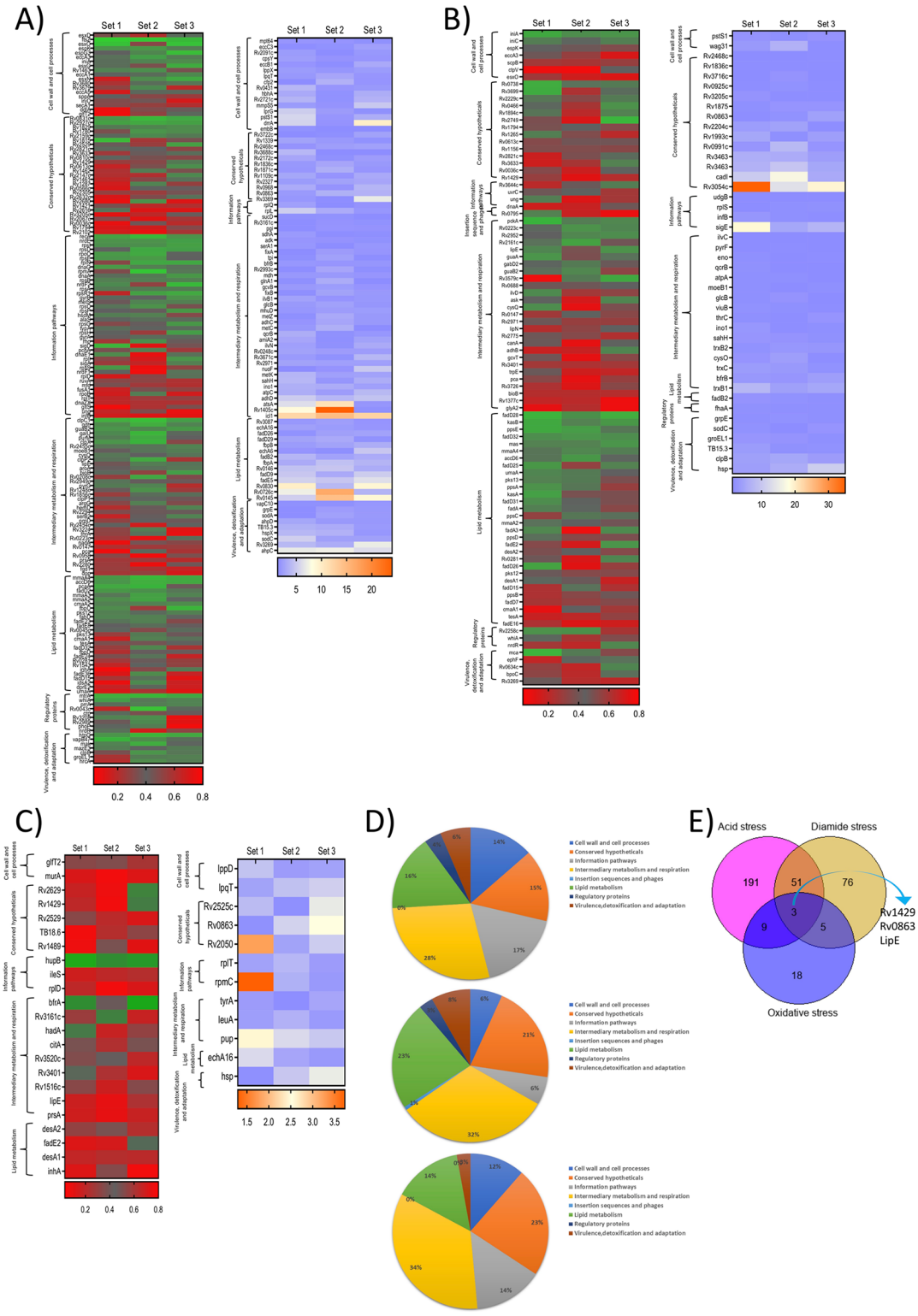

Figure 3. Quantitative global proteome analysis of mycobacteria treated with different stress agents. (A–C) Heat map depicting the fold-difference in the expression of proteins that are differentially regulated upon bacterial exposure to acid (A), diamide (B), and H_2O_2 (C) compared to untreated bacteria across the three biological replicates. (D) Percentage distribution of DEPs corresponding to various functional categories under multiple stresses. (E) Pie chart showing Mtb proteins that are commonly regulated in response to acidic, diamide, and oxidative stresses. Total proteins altered under each of these conditions were used for comparative analysis.

virulence, detoxification, and adaptation (3%). These analyses further reveal that during acidic stress at pH 5.5, functional categories that largely comprised upregulated proteins include intermediary metabolism and respiration (n = 35/88), whereas maximum proteins that are repressed belong to information pathways (n = 42/167). Likewise, under diamide stress most induced proteins are those involved in intermediary metabolism and respiration (n = 16/44) or some unknown functions (n =

https://doi.org/10.1021/acsomega.2c03092
ACS Omega 2022, 7, 26749−26766

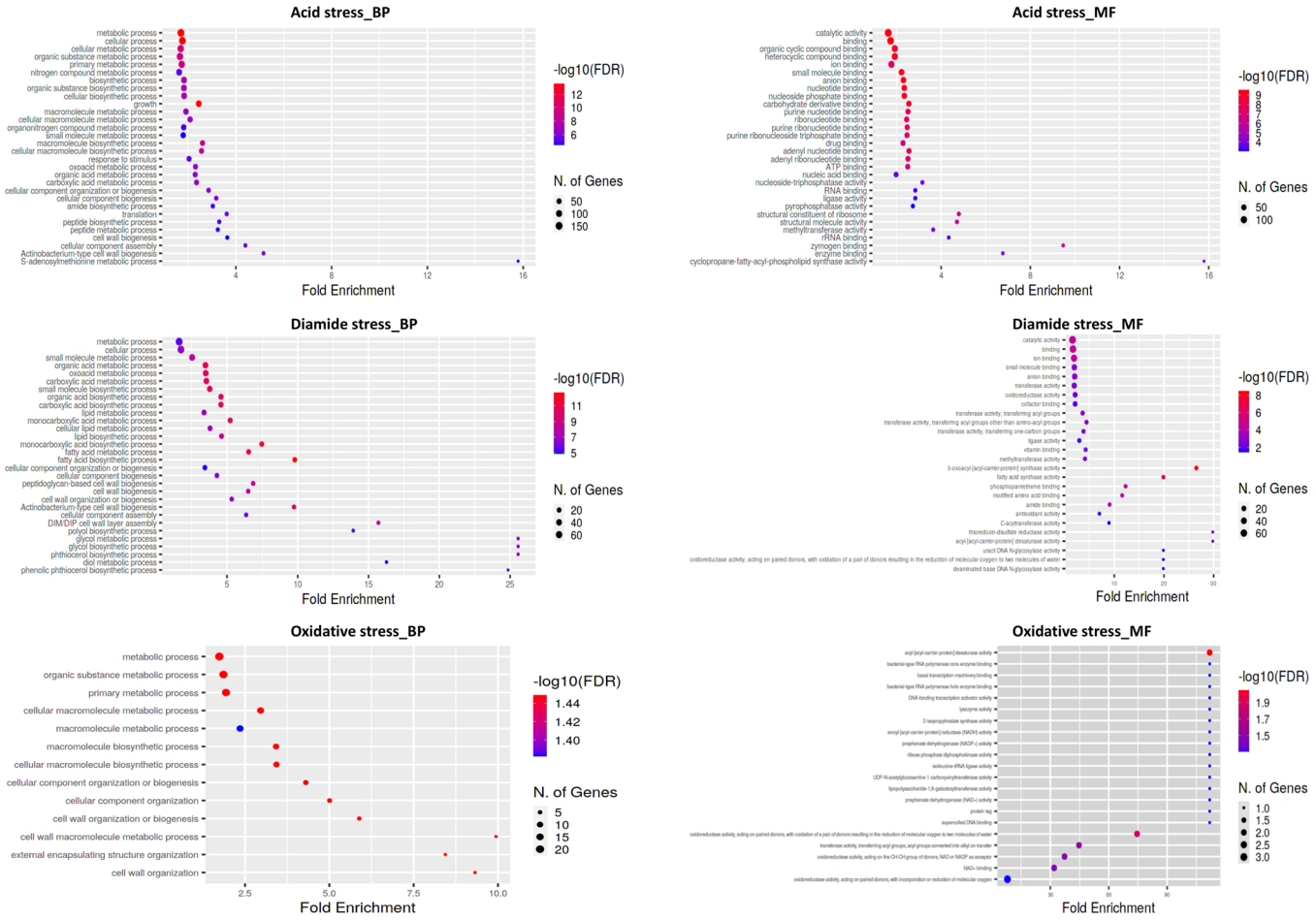

Figure 4. GO enrichment analysis of stress-regulated proteins. GO enrichment analysis of DEPs was performed using ShinyGO v0.741 based on the BP and MF identified under different stress conditions. Shown are the number of DEPs as spots belonging to top 30 hallmark pathways. The spot size represents the number of genes corresponding to regulated proteins and spot color indicates FDR as *p*-values. *X*-axis denotes the enrichment factor of differentiated proteins.

14/44), whereas proteins undergoing downregulation are primarily those related to the lipid metabolism function (n = 30/91) or intermediary metabolism and respiration (n = 27/91). In contrast to the acid and diamide stresses, H_2O_2 treatment resulted in upregulation of a small set of 12 proteins uniformly distributed across six functional classes, whereas proteins involved in intermediary metabolism and respiration (n = 9/23) are primarily downregulated. Overall, these data reveal a distinct set of proteins modulated under different in vitro conditions of Mtb growth simulating the intracellular environment (Figure 3A–D).

To find out the integrative stress response of mycobacterium, we also determined the common proteins that are regulated under physiological changes brought by acidic, diamide, and H_2O_2 stresses. A considerable number of proteins common between acid and diamide stress are noticed. Of these, 33 proteins are downregulated in both stresses, while 13 proteins are commonly upregulated (Table S2). In addition, we find few proteins (MoeB1, Rv3205c, ClpB, InfB, GroEL1, FadD26, and Rv2971) that are commonly present but show a distinct expression pattern between both stresses. Interestingly, three proteins viz. probable lipase LipE (*Rv3775*) related to lipid metabolism, conserved protein Rv1429, and uncharacterized protein Rv0863 are found to exhibit a similar pattern of expression under all three stress conditions (Figure 3E). While LipE and Rv1429 are downregulated, expression of Rv0863 is upregulated upon exposure to all three stress agents (Table S1). Next, we validated the expression profile of a few candidate proteins under these stresses by immunoblotting. We randomly probed PknB which is induced by 2.1-fold by acid and 1.6-fold by H_2O_2 treatments and HtpG and FadA exhibiting 0.16-fold and 0.42-fold reduction following exposure to acid and diamide, respectively (Table S1). As shown in Figure S2, immunoblotting with the help of specific antibodies shows a similar trend, as observed by mass spectrometry, in all three replicates, thus corroborating the proteomic data.

Overall, these findings suggest a well-coordinated and condition-specific response of mycobacterium to varied in vitro stresses leading to global remodeling of proteome.

Functional Annotation and Enrichment Analysis of Identified Differential Proteins. To further comprehend the functional annotation and properties of these regulated proteins, we analyzed the data sets using the ShinyGO v0.741 online server based on annotations from STRING-db(v.11). To ascertain the GO classification, terms BP and MF were utilized. The differentially regulated proteins were considered over-represented with a positive fold enrichment value ($p < 0.05$) and were linked with different BPs and MFs, as classified by GO annotation.

https://doi.org/10.1021/acsomega.2c03092
ACS Omega 2022, 7, 26749−26766

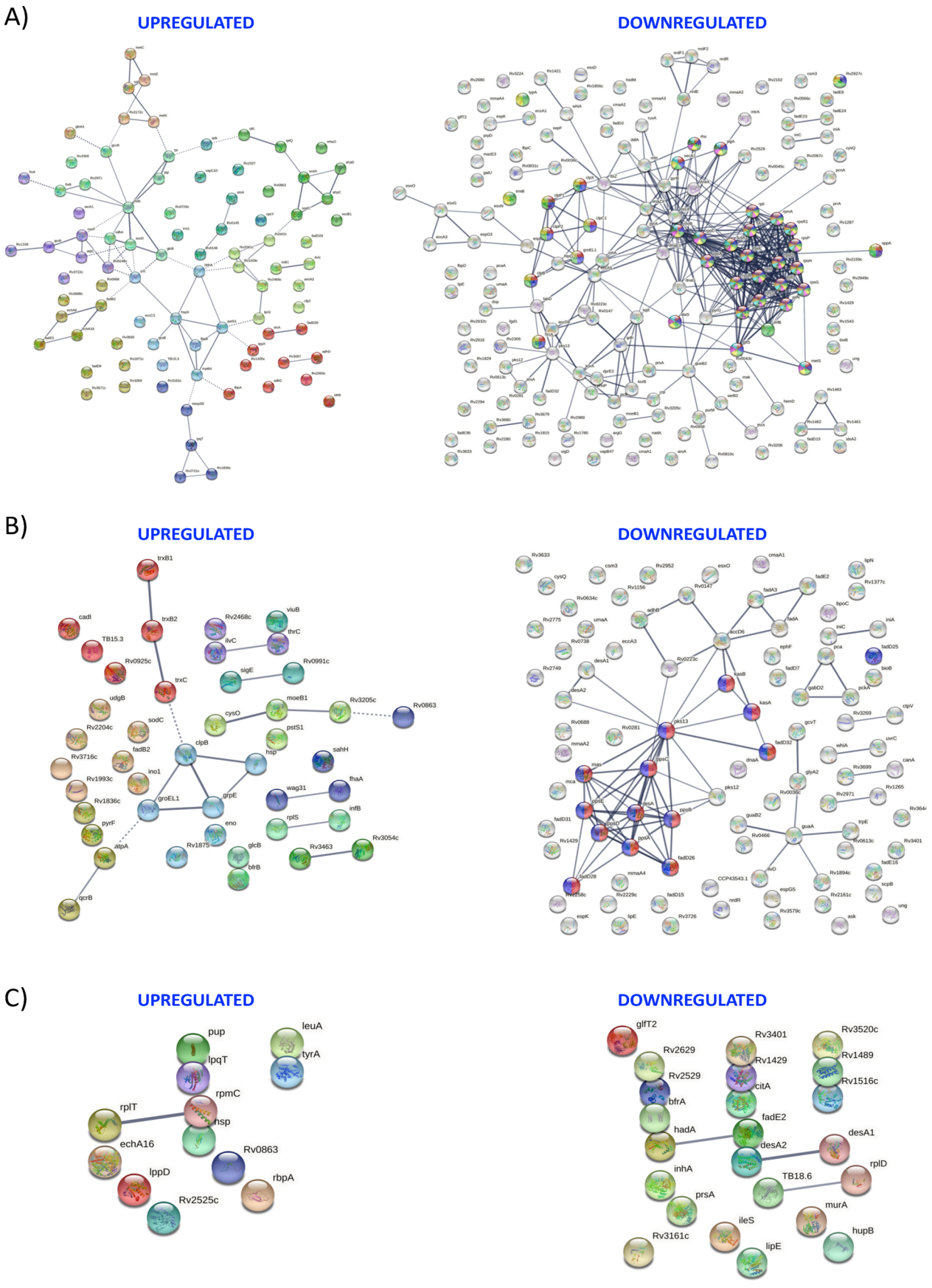

Figure 5. PPI network of mycobacterial proteins under stress conditions. Network plot of up- and downregulated proteins, identified during acidic stress (A), diamide stress (B), and oxidative stress (C), predicted by STRING. Lines represent linkages that exist between proteins, having a confidence score of 0.7 and identical colored bubbles represent the local network cluster of proteins.

https://doi.org/10.1021/acsomega.2c03092
ACS Omega 2022, 7, 26749−26766

A)

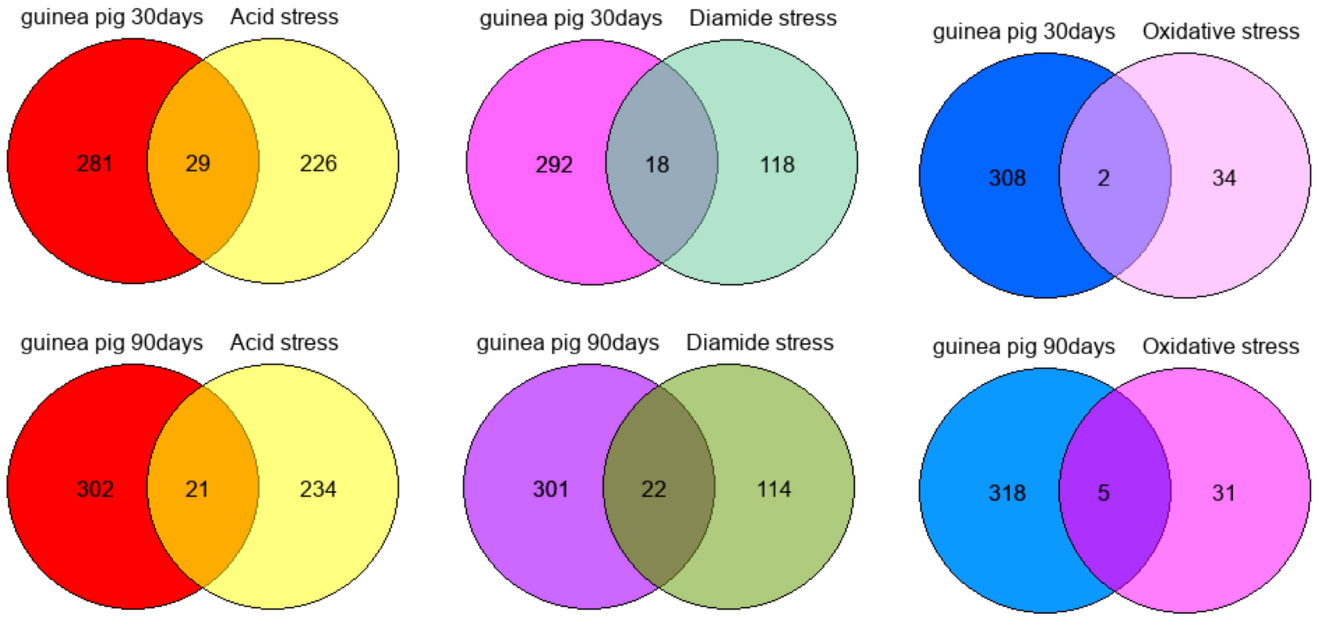

B)

Guinea pig 30 day infection vs Acid stress		Guinea pig 90 day infection vs Acid stress		Guinea pig 30 day infection vs Diamide stress		Guinea pig 90 day infection vs Diamide stress		Guinea pig 30 day infection vs Oxidative (H2O2) stress		Guinea pig 90 day infection vs Oxidative (H2O2) stress	
Locus	Name	Locus	Name	Locus	Name	Locus	Name	Locus	Name	Locus	Name
Rv0672	fadE8	Rv3800c	pks13	Rv0863	Rv0863	Rv3800c	pks13	Rv0863	Rv0863	Rv3808c	glfT2
Rv0863	Rv0863	Rv3318	sdhA	Rv2940c	mas	Rv2940c	mas	Rv1484	inhA	Rv1484	inhA
Rv2967c	pca	Rv3808c	glfT2	Rv2967c	pca	Rv1679	fadE16			Rv1899c	lppD
Rv0993	galU	Rv0724	sppA	Rv2187	fadD15	Rv3726	Rv3726			Rv3401	Rv3401
Rv2476c	gdh	Rv3139	fadE24	Rv2933	ppsC	Rv0020c	fhaA			Rv3710	leuA
Rv3318	sdhA	Rv3003c	ilvB1	Rv0145	Rv0145	Rv2933	ppsC				
Rv2187	fadD15	Rv0952	sucD	Rv0343	iniC	Rv0934	pstS1				
Rv0711	atsA	Rv1484	inhA	Rv0342	iniA	Rv3879c	espK				
Rv2950c	fadD29	Rv0934	pstS1	Rv1837c	glcB	Rv1837c	glcB				
Rv0145	Rv0145	Rv2376c	cfp2	Rv2131c	cysQ	Rv1836c	Rv1836c				
Rv2555c	alaS	Rv3879c	espK	Rv0189c	ilvD	Rv1259	udgB				
Rv1484	inhA	Rv1837c	glcB	Rv1023	eno	Rv3396c	guaA				
Rv0667	rpoB	Rv1836c	Rv1836c	Rv0969	ctpV	Rv3401	Rv3401				
Rv1248c	Rv1248c	Rv1832	gcvB	Rv2941	fadD28	Rv0001	dnaA				
Rv0343	iniC	Rv0284	eccC3	Rv0761c	adhB	Rv0969	ctpV				
Rv0342	iniA	Rv0001	dnaA	Rv2934	ppsD	Rv2928	tesA				
Rv1837c	glcB	Rv2461c	clpP1	Rv2932	ppsB	Rv2246	kasB				
Rv2131c	cysQ	Rv1798	eccA5	Rv2931	ppsA	Rv2245	kasA				
Rv3676	crp	Rv2928	tesA			Rv2934	ppsD				
Rv1020	mfd	Rv2247	accD6			Rv2932	ppsB				
Rv2243	fabD	Rv2936	drrA			Rv2931	ppsA				
Rv0905	echA6					Rv2247	accD6				
Rv3869	eccB1										
Rv1547	dnaE1										
Rv2981c	ddlA										
Rv3596c	clpC1										
Rv3868	eccA1										
Rv2363	amiA2										
Rv2936	drrA										

Figure 6. Meta-analysis of regulated proteins. (A) Venn diagram representing the mycobacterial proteins that are commonly regulated (up- or downregulated) during in vitro stress conditions and in vivo Mtb challenge is shown. The protein data set from the 30- and 90-day guinea pig infection study is compared with differential protein signatures captured under stress conditions in this study. (B) Locus and gene identification of DEPs common to the guinea pig infection study are listed.

The top 30 GO terms based on BP and MF, ranked by the number of genes present in the high-level GO category and fold-enrichment score, are presented in Figure 4. By enrichment analysis, we observe that under acidic and diamide stresses, the set of maximum regulated proteins predominantly belong to metabolic BP (n = 153 for acid and n = 77 for diamide stress) and catalytic activity MF (n = 136 for acid and N = 71 for diamide stress) (Figure 4). Likewise, a distinct pattern of enrichment is observed under the oxidative stress conditions, where proteins are highly associated with metabolic BP (22) and binding MF (17) (Figure 4).

https://doi.org/10.1021/acsomega.2c03092
ACS Omega 2022, 7, 26749−26766

The enrichment analysis ranked by fold-enrichment reveals that acidic stress-defining proteins are related to Actinobacterium-type cell wall biogenesis BP (fold = 5.48) and MF viz. cyclopropane-fatty-acyl-phospholipid synthase activity (fold = 15.79) (Figure 4). Similarly, in the diamide protein set, the top-ranked BP and MF based on fold-enrichment are the glycol metabolic process (fold = 25), glycol biosynthetic process (fold = 25), phthiocerol biosynthetic process (fold = 25), and thioredoxin-bisulfide reductase activity (fold = 29.8) and acyl-[acyl-carrier-protein] desaturase activity (fold = 29.8), respectively (Figure 4). The top-ranked BPs associated with H_2O_2 stress are cell wall organization (fold = 9.3) and cell wall macromolecule metabolic process (fold = 9.9), and enriched MF terms include acyl (acyl-carrier-protein) desaturase activity, basal transcription machinery binding, DNA binding activity, prephenate dehydrogenase activity, lysozyme activity, ribose phosphate diphosphokinase activity, and isoleucine-tRNA ligase activity (fold = ∼111) as well as other functions (Figure 4). Overall, these results suggest that proteins inflicted in mycobacterium stress response majorly participate in an array of metabolic processes, and catalytic and binding functions.

Interaction Network Analysis of DEPs Identified during Stress in Mtb. The PPI networks were constructed for DEPs using STRING, and all the up- and downregulated proteins from different stresses were mapped to the interaction database (Figure 5). The association among seed proteins was predicted at a high confidence level of >0.70, based on functional-physical correlation, lab experiments, and knowledge derived from curated databases, and is represented by the edges. As shown in Figure 5, closely linked proteins grouped as clusters were interpreted within these networks.

During acidic stress (Figure 5A), the upregulated proteins involved in amino acid metabolic and catabolic processes (brown bubbles); oxidative phosphorylation and t-RNA processing activity (light green bubbles); tricarboxylic acid (TCA) cycle, pentose phosphate pathway, oxidation of organic compounds, drug metabolic process, precursor metabolite and energy generation (light blue bubbles); antioxidant activity, cellular detoxification and response to toxic substance (yellow bubble); cellular response to starvation, external stimuli and nutrient levels (red bubbles); efflux transporters, lipid homeostasis, cell activation involved in immune response and amino acid metabolic process (crystal green bubbles); regulation of T-cell function and phospholipids, glycolipid binding (dark green bubbles); peptide metabolic and biosynthetic process, translation, and purine nucleotide salvage (purple bubbles) are highly interconnected. Among the downregulated proteins under acid treatment, most of the clusters found in PPI network analysis are related to BPs such as the nucleotide biosynthetic process, DNA metabolic process, and cellular macromolecule process (yellow bubbles); zinc ion and inorganic cation homeostasis, toxin protein secretion and virulence (crystal green); response to stress, superoxide and temperature stimulus, proteolysis and nucleoid organization (light green bubbles); fatty acid, lipid biosynthetic and metabolic process, cell wall biogenesis and cellular developmental process (purple bubbles); nucleotide metabolic and biosynthetic process (red bubbles); iron−sulfur cluster assembly and protein processing (light blue); cellular macromolecule and nucleic acid metabolic process, organelle organization and DNA conformation change (dark green); peptide metabolic and biosynthetic process, translation and macromolecule biosynthetic process (dark blue); and TCA metabolic process, cellular respiration and glutamate catabolic process (brown bubbles), respectively (Figure 5A).

Furthermore, network analysis of upregulated proteins from diamide stress (Figure 5B) reveals that protein folding, response to extracellular stimulus and cell communication (light blue); cellular response to oxidative stress, toxic substance and chemical stimulus, cellular detoxification and homeostasis (red bubbles); and cysteine, serine, and sulfur amino acid biosynthetic and metabolic process (light green bubbles) proteins are interconnected (Figure 5B). Also, the clusters of downregulated proteins were correlated with fatty acid, lipid, and organic acid biosynthetic process, fatty acid and lipid metabolic process (white bubbles); TCA, pentose phosphate and oxidative phosphorylation pathways and malonyl-CoA metabolic process (white bubbles); glycol, diol, and polyol biosynthetic and metabolic process, and cell wall layer assembly and cell wall biogenesis (red-blue bubbles) related responses (Figure 5B). In case of the oxidative process, no specific backbone of the interaction network is revealed, suggesting that the target proteins share no overlapping function (Figure 5C). Collectively, the above PPI network analyses illuminate major BPs that are modulated in the virulent Mtb pathogen during its confrontation with multiple stress conditions and provide adaptive capacity to face the intracellular hostile conditions.

Proteome-Wide Prediction of Mtb Proteins That Are Significant in Host Stress Response. To further identify proteins that are modulated (up- or downregulated) during in vitro stress as well as in the intracellular pathogen during infection, we compared the Mtb proteome data sets obtained from mammalian lungs[30] with the expression signatures acquired as a response to stresses on the in vitro cultured Mtb in this study. We find that 29 DEPs identified in the guinea pig 30-days infection model are common to our acidic stress condition analysis. Likewise, 21 proteins overlap with the 90-days guinea pig infection model. Similar comparison led to the identification of 18 and 22 proteins regulated under diamide stress that are common to 30- and 90-days guinea pig infection models, respectively. In addition, two and five proteins specific to H_2O_2-mediated oxidative stress are also found in the in vivo data set of 30-and 90-days guinea pig infection models, respectively. An overlap between the in vitro model of stress conditions and in vivo infection studies reveals the apparent set of proteins that are critical for maintaining the physiology of intracellular pathogens to rapidly adapt and survive in hostile host conditions (Figure 6A,B).

DISCUSSION

In this study, we aim at identifying the specific changes associated with in vitro acidic and oxidative stress environments in Mtb $H_{37}Rv$ by using iTRAQ-based quantitative proteomics. The quantitative proteomics approach has been instrumental in understanding the sensitivity and adaptive potential of different pathogens to the imposed stresses during intracellular infection.[31−34]

The most enticing fact about mycobacterium as an intracellular pathogen is its ability to manage metabolic and environmental adversities tossed by the host. These diverse host conditions trigger survival and adaptive responses within mycobacterium, making it important to understand the stress responses and their regulation and pathological relevance. There are a plethora of conditions inside infected macrophages such as hypoxia, nutrient scarcity, low pH, and reactive oxygen and nitrogen species that stimulate mycobacterium physiological

https://doi.org/10.1021/acsomega.2c03092
ACS Omega 2022, 7, 26749−26766

adaptive responses and resistance mechanisms toward these immune pressures.[35] To understand the intracellular context of strategies used by Mtb for its survival and persistence inside the host, several studies have been conducted in recent years using transcriptomics.[36−39] However, due to inconstancy in the turnover ratio of mRNA and protein, primarily because of post-transcriptional modifications,[40] it is vital to characterize the bacterial proteomic response to different intracellular stress conditions. To fill the knowledge gap from prior studies where emphasis was largely on quantitation of transcripts, herein we performed a comprehensive study in which we opted for in vitro stress models mimicking oxidative and acidic intracellular environments. Our focus was mainly to delineate the protein signatures that are distinctive for defense against these stresses, and hence to create a theoretical basis for future mechanistic studies. The proteomic data from three biological replicates for all three stress conditions reveal only a fraction of total proteins that are consistently modulated (Figure 2C). The apparent variability among the biological replicates could be due to the transient change in the expression profile of several of the Mtb proteins. Nonetheless, we found a significant number of proteins that were consistently altered across the three biological replicates, thus indicating their specific response to the respective stress condition. Such proteins were considered for further analysis to construe the landscape of Mtb proteome upon exposure to acidic and oxidative stress environments.

Mtb H_{37}Rv Proteomic Response to Acidic Stress. Mtb resides in the acidified environment during infection and experiences different pH as it is trafficked through mildly acidic phagosomes of resting macrophages (pH 6.1−6.4) and fully acidic phagolysosomes in activated macrophages (pH 4.5−5.4).[41] We chose the experimental condition of pH 5.5 in acidic stress (Figure 1B) to mimic the possible early infection stage inside macrophages. There is evidence suggesting survival competence of mycobacterium in acidic and degradative environment of vacuoles.[13,42] Mtb regulates its growth at acidic pH under different culture conditions like in the presence of Sautons medium or different carbon sources.[13] Our results showed optimal growth in rich medium viz. 7H9 containing oleic acid and glycerol until day 4 postinoculation at pH 5.5, indicating the physiological flexibility of Mtb against growth restrictions known to be imposed by phagolysosome acidic conditions (Figure 1B). Several studies have demonstrated the physiological changes in the transcriptome of Mtb following phagocytosis, supporting the notion of resistance and adaptive mechanisms active against pH-driven antimicrobial properties of macrophage phagosomes.[43,44] The global profile of Mtb H_{37}Rv proteome under acidic pH, in the current study, serves as an extensive node to these earlier data sets that bore testimony of the dynamic response of Mtb during this stress.

The iTRAQ-based mass spectrometry reveals that acidic stress majorly induces multilayered responses in Mtb H_{37}Rv that are specific to metabolism, cellular respiration, macromolecule biosynthesis and repairing, cell wall biogenesis, proteolysis, translation, and virulence (Figures 3 and 4). We observed modulation in the expression of proteins that are part of branched chain fatty acid metabolism. The activation of Icl and GlcB that are attributed to anaplerotic node[45] of TCA suggests that under an acidic environment, Mtb undergoes metabolic shift to allow utilization of fatty acids for cellular growth. The upregulation of glyoxylate cycle enzymes during the macrophage[46] and mouse infection model[47] further strengthens the essentiality of these enzymes during host infection. Moreover, the increased expression of SucD, SdhA, and Mdh (Figure 3A) suggests that Mtb utilizes the reductive TCA cycle (rTCA) for anaerobic carbon fixation and to support its intracellular growth under low-pH conditions.[48] This survival strategy is also adopted by other intracellular pathogens, including *Helicobacter pylori* and *Salmonella enterica* to facilitate their persistence and distribution across host niches during oxygen-limiting conditions.[49] The suppression of methylcitrate dehydratase-PrpD protein (Figure 3A), involved in propionate metabolism via methyl citrate cycle, alleges that low pH triggers rewiring of central carbon metabolism and supports that fatty acid catabolism is required by Mtb for in vivo growth and pathogenesis.[46,50]

The acidic pH condition in the extracellular milieu causes a change in proton flux through the cell membrane thereby demonstrating acid tolerance response.[51] It is also shown that Mtb at acidic pH experiences reduced cytoplasmic potential[52] which may cause enhanced generation of reactive oxygen species (ROS) and induction of oxidative stress.[53] Remarkably, the release of antioxidant molecules triggered by acidic stress has been demonstrated in *Staphylococcus aureus*,[54] *Streptococcus. mutans*,[55] *Lactococcus lactis*,[54] *Vibrio vulnificus*,[56] and *Bacillus cereus*[57] together suggesting the possible overlap in the physiology of acid and oxidative stresses across different bacteria. Interestingly, we also observed the activation of superoxide dismutases, SodA and SodC proteins under acidic pH, thus implying the detoxification of free radicals generated during acidic stress in Mtb (Figure 3A). In addition, induction of alkylhydroperoxide reductases viz. AhpC and AhpD in our data set, identified as key elements of Mtb antioxidant defense system,[58] emphasizes on the role of these enzymes in conferring survival advantage to Mtb against acidic stress. Another interesting class of proteins found activated under acidic pH conditions belongs to cellular iron homeostasis. Sensing the in vitro low pH as acidic and hydrolytic conditions similar to those impounded by phagolysosome, Mtb responds by regulating the iron acquisition and storage machinery. Our data show increased expression of membrane protein MmpS5, which facilitates internalization of ferric iron from the host by assisting the export of iron chelators called siderophores across the cell envelope.[59] Altered expression of iron storage protein BfrB, a bacterioferritin,[60] and heme storage protein MhuD, an oxygenase,[61] upon acidic stress suggests their role in instigating the acidic stress response during intracellular growth, as reported earlier.[39] Altogether, the differential regulation of iron homeostasis under acidic conditions implies activation of iron-mediated regulatory circuits as a strategy to adapt the stressful environment (Figure 3A). Because oxidation of the endogenous iron pool is an environmental cue for pathogens to initiate the adaptive response, it would be interesting to know that oxidative stress initiated by acidic pH is directly responsible for activating molecular components involved in iron homeostasis.

Furthermore, we observed the induction of Rv3671c, annotated as MarP, under low-pH conditions (Figure 3A), which provides resistance to acidic stress and helps pathogen survive inside phagolysosomes and during infection in macrophages and mice.[13,62] The induction of MarP, thereby, suggests that the acid tolerance system is intact in Mtb at this time point. Interestingly, we also discovered the differential expression of response regulator PhoP, a member of *PhoPR* regulon (Figure 3A). Studies have proven the role of this two-component system in carbon-source-mediated slow growth at acidic pH, in maintaining redox homeostasis,[63] in inducing expression of

https://doi.org/10.1021/acsomega.2c03092
ACS Omega 2022, 7, 26749−26766

acidic pH-responsive virulence factors, and in lipid anabolism.[64] In contrast to these roles of PhoPR-dependent low-pH adaptation, we find repression of the PhoP component at pH 5.5. The activation of the glyoxylate shunt pathway under acidic conditions (Table S1) and downregulation of PhoP together suggest the involvement of PhoPR-independent adaptation to acidic pH conditions by promoting remodeling of metabolism for sustainable growth.

The acidic pH is detrimental for the structural stability of cellular macromolecules. The condition of acidic pH causes disruption of protein folding due to high protonation of amino acid residues.[65] In addition to protein, DNA is also vulnerable to the attack by acidic pH at low pH.[66] We noticed downregulation of proteins majorly involved in repairing and maintaining the integrity of these macromolecules. A number of proteins involved in DNA conformational change (GyrA and GyrB) and DNA damage repair (RecA, RuvA, and DnaE1) were found to be downregulated. In addition, proteins participating in proteolysis (ClpP1, ClpP2, ClpX, and ClpC1) and proteostasis (GroEL1, ClpB, and htpG) machinery were also repressed (Figure 3A). The role of chaperonins in maintaining stable proteome under numerous stresses, including acidic pH, is widely studied in *E. coli*,[67] *S. mutans*,[68] *Listeria monocytogenes*,[69] and *S. pneumoniae*.[70] Surprisingly, downregulation of cytoplasmic chaperones and Clp machinery in Mtb that are quintessential for proteome homeostasis under stress indicates that acidification does not result in protein unfolding or denaturation, directly. In addition, a considerable number of ribosomal proteins that constitute 50S (RplN, RplI, RplD and RplT) and 30S (RpsL, RpsD, RpsE, RpsB, RpsA, RpsR1, RpsC, RpsP, RpsG, RpsH, and RpsS) ribosomal subunits showed reduced expression (Figure 3A), which is in line with the transcriptional response of Mtb toward NO and ROS stress.[37,71] This might be due to the cessation of the ribosome production thereby repressing the translational process. Not only this, proteins involved in DNA replication (DnaA, DnaG, and DnaZX) were also seen repressed in our study. It is anticipated that mycobacterium ensures the accurate DNA synthesis and replication under the stressful conditions.[72] The slowdown of translational and transcriptional machinery indicates that after sensing the environmental cues, Mtb undergoes physiological adaptation and creates an energy balance by switching its metabolism. Altogether these observations represent that bacterium is in a state of adaptive trends, most likely on an energy-saving mode.

Whole Cell Proteomic Response of Mtb $H_{37}Rv$ to Oxidative Stress. Here, we defined the broader notion of oxidative stress by identifying the regulatory proteins in response to both H_2O_2 and disulfide stress. Diamide, a known oxidant for thiols,[73] was used to mimic the physiological scenario during infection where mycobacterium is exposed to the toxic environment of host-generated reactive species via oxidative burst.[74] The differential set of proteins exclusive to diamide treatment signify that disulfide stress is not only the branch of oxidative stress, but it also affects a complex of molecular networks.[75] Interestingly, we found activation of antioxidant enzymes viz. TrxB1, TrxB2, and TrxC that are key players of the thioredoxin system in Mtb (Figure 3B)[76] and are implicated in thwarting the oxidative stress in several organisms.[77,78]

As shown in a previous transcriptomic study,[37] here we have seen the stimulation of GroEL1, GrpE, ClpB, and Hsp proteins along with SigE sigma factor, which reveals the involvement of a repertoire of chaperonins under the oxidative stress condition as a resistance mechanism against proteotoxic stress (Figure 3B). Remarkably, GroEL1 and ClpB were downregulated in our study during acidic pH conditions implying the stress-specific functional modality in regulators of host-adaptive mechanisms. Not only in diamide stress, GrpE is shown to be actively involved in Mtb under heat shock and hypoxia stresses as well, thus indicating the overlap of effector molecules in protecting Mtb against different stressors.[79]

We also report the induction of proteins viz. Thiocarboxylate CysO, a member protein in *mcc* operon which is involved in the cysteine biosynthesis salvage pathway[80] and MoeB1 a rhodanese-like protein involved in molybdopterin synthesis (Figure 3B).[81] Our results are in coherence with a previous study which showed differential expression of *moeB1* and *cysO* Mtb transcripts under redox stress in a *clgR*-dependent manner.[82] It is interesting to find out that MoeB1 (also annotated as MoeZR) also participates in the sulfuration of CysO,[81] thus suggesting a possible link between cysteine biosynthesis, molybdenum biosynthesis, and sulfur homeostasis pathways under redox conditions. The fact that cysteine has a role in Mtb pathogenesis via immunity against reactive species[83] creates premises for role of these proteins in maintaining the redox homeostasis during macrophage survival.

When it comes to survival under an adverse host environment, cell envelope architecture of Mtb plays a significant role.[84−86] The proteomic profile of stressed Mtb shows that proteins belonging to PDIM operon viz. FadD26, PpsA, PpsB, PpsC, PpsD, PpsE, Mas, and FadD28 are downregulated upon exposure to diamide (Figure 3B).[87] A similar pattern of downregulation was observed at the transcript level of these genes in the nutrient starvation model.[88] It is conceivable that like starvation conditions, diamide-mediated thiol oxidative stress also causes modulation in the cell wall lipid composition via differential expression of these polyketide and nonribosomal peptide synthesis-based proteins. In a study by Singh et al., it was revealed that synthesis of virulence lipids in Mtb is dependent on the redox atmosphere inside macrophages. The differential lipid profiles were observed after exposure to diamide or DTT and the metabolic shift was seen toward poly acycl trehaloses (PAT), PDIM, and TAG synthesis under respective treatment conditions.[89] While we observe downregulation of PDIM synthesis and transport during diamide treatment, we do not find activation of an alternative pathway for the synthesis of other cell wall components such as PAT, di-acyltrehaloses, or sulfolipids (SL-1), suggesting that either additional factors are involved in fatty acid anabolism during redox imbalance or Mtb is under nonreplicating conditions shutting down its lipid anabolism in response to disulfide stress.

In addition, enzymes required in mycolate biosynthesis, transport, and modification were also regulated upon diamide treatment.[90] The expression of FadD32, Pks13, beta ketoacyl synthases KasA and KasB, methyltransferase MmaA2 and MmaA4, and cyclopropane synthase CmaA1 was found suppressed (Figure 3B), which together suggest that Mtb modulates the mycomembrane composition while responding to thiol-stress conditions. Interestingly, the perturbations in the intracellular levels of FabD, AccD6, MmaA2, MmaA3, MmaA4, CmaA1 and CmaA2, PcaA, FadD32 and Pks13, and FbpC and FbpD were also seen during acidic pH conditions in our study (Figure 3B). It is indicative that the manipulation of cell wall biogenesis under acidic and thiol oxidative stresses by decreasing the expression of PDIMs and mycolic acid might support the

https://doi.org/10.1021/acsomega.2c03092
ACS Omega 2022, 7, 26749−26766

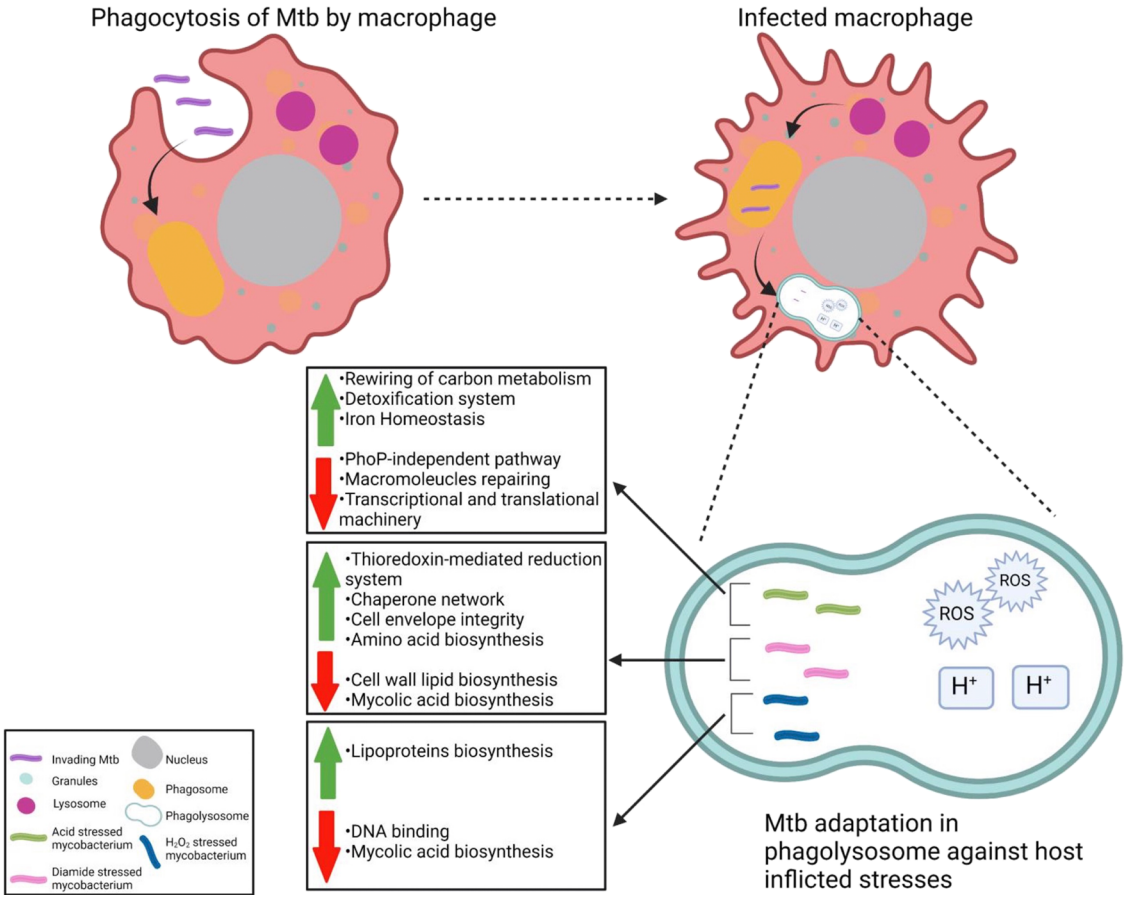

Figure 7. Model depicting the physiological adaptation of Mtb under hostile environment inside phagolysosomes of infected macrophages. In vitro stress treatment viz. acidic, diamide (thiol-oxidants), and H_2O_2 (OH^-) causes differential regulation of many biological processes and adaptive redirecting of the mycobacterium proteome. Created with Biorender.com.

pathogen in attaining the persister-like phenotype while still preserving its virulence.[91] These results are in agreement with the transcriptome data showing suppression of mycolic acid biosynthesis during prolonged infection of resting macrophages by Mtb.[38] The fact that mycolic acid molecules are stable even after 96 h of starvation[90] suggests that mycobacterium relies on energy-saving mode by slowing down the mycolic acid biosynthesis, which serves as a righteous approach for adaptive response to acidic and thiol oxidative stress conditions.

Under aerobic growth conditions, the auto-oxidation of enzymes containing flavins, quinones, and other respiratory enzymes are the chief intracellular sources of ROS viz. superoxide and peroxide.[92] Upon infection, Mtb experiences the inhibitory effect of reactive oxygen and nitrogen species produced during oxidative burst inside macrophages.[93] Hydroxyl radicals are the most reactive ROSs produced from peroxides by the Fenton reaction, which causes oxidative damage to macromolecules including lipids.[94] Here, we studied the proteomic response of Mtb to oxidative agent H_2O_2 to identify the cellular consequences against ROS. Our data did not show induction of many classic proteins that are known to regulate the H_2O_2 response and have been identified crucial in the oxidative stress detoxification mechanism.[93] One of the possible reasons could be the high basal expression levels of several associated proteins, as depicted for KatG and AhpC.[37] It is quite evident that Mtb shows resistance against host immune responses through its impermeable cell envelope. Lipoprotein forms an important constituent of the bacterial cell envelope, playing an essential role in drug export, antibiotics action, and cell wall homeostasis.[95,96] The role of lipoprotein-synthesis and modifying enzymes in bacterial virulence is well documented in *S. aureus*[97] *and Enterococcus faecalis*.[98] Similarly, Mtb lipoprotein signal peptidase (*lspA*) is essential not only in the virulence of Mtb, but its expression is also regulated in the acidic and surface stress.[99] In support of the role of lipoproteins in intracellular survival, we saw upregulation of LpqT and LppD proteins under H_2O_2-mediated oxidative stress (Figure 3C). An upregulation of lipoprotein LpqT is in agreement with a previous study with *M. smegmatis* where *lpqT* was shown to be required for survival under low pH and oxidative stress.[100] Moreover, LpqT-mediated defects in Mtb antigen presentation to $CD4^+$-T cells may provide a mechanism by which this protein supports the pathogen for intracellular survival under stress conditions.[100] Another interesting protein found regulated in H_2O_2 stress is HupB. DNA binding proteins are crucial in maintaining the structure and organization of chromosomal DNA in response to genotoxic stress. In particular, nucleoid-associated proteins including HU (histone-like proteins), H-NS (histone-like nucleoid structuring protein), and IHF (integration host factor) function as modulators in maintaining the nucleoid dynamics under unfavorable conditions,[101,102] either by regulating gene expression or by maintaining topological changes in the chromosome. HupB, a HU protein, manifests its effect in virulence,[102] SOS response, and stress response across bacterial species.[103] Many studies have shown the participation of HupB in protecting DNA from free hydroxyl radicals in *Francisella*

https://doi.org/10.1021/acsomega.2c03092
ACS Omega 2022, 7, 26749−26766

tularensis[104] and its regulatory role in *Heliobacter pylori* against acidic stress by preventing endonucleolytic cleavage of DNA.[105] Contrary to these bacteria, expression of *hupB* along with a few other NAP-encoding transcripts was unaffected in Mtb upon oxidative stress.[106] Notably, our proteomic data show down-regulation of HupB after H_2O_2 treatment. Results from our study provide credence to the idea that Mtb prefers metabolic arrest overactive defense mechanism to combat oxidative stress.

Remarkably, among several DEPs, we identified three proteins viz. Rv0863, Rv1429, and LipE that are modulated upon exposure to all three stress conditions (Figure 3E). It is assumed that putative lipases encoded by Mtb genome may be involved in hydrolysis of long-chain acylglycerols in order to release fatty acids from stored host lipids.[107] Mtb relies on the activity of these lipases that are part of the Lip family, during the course of infection. Studies have shown that lipases are required by Mtb for infection and persistence in the host.[108,109] However, our data showed suppression of LipE protein upon exposure to acid and oxidative stresses. Taking into consideration the role of LipE in lipid catabolism and the downregulation of fatty acid and lipid synthesis as well as transport under multiple stresses (Figure 3), it appears that mycobacterium adapts to these extracellular conditions by slowing down the metabolic and synthesis pathways and eventually undergoes dormant-like conditions. The upregulation of conserved hypothetical proteins Rv0863 and downregulation of conserved protein Rv1429 under all three stress conditions warrants future studies to characterize their role in Mtb pathogenesis and intracellular survival. In addition, our data set includes a small subset of stress proteins including the general stress protein Rv0863 that are also modulated during the guinea pig infection model at both early and late time points of infection (Figure 6A,B).[30] Future studies are warranted to establish a direct role of some of these in Mtb virulence and growth inside host cells, which can further help us identify potential anti-TB drug targets.

Overall, this study offers a global proteome profile of Mtb under acidic-, diamide-, and H_2O_2-mediated stress conditions. As summarized in Figure 7, differentially regulated proteins present a dynamic response of Mtb to acidic and oxidative stress. Moreover, the overlap between acidic and oxidative stresses is suggestive of the adaptive response of the pathogen to intracellular stresses and preparing itself to face multitude of forthcoming adverse host conditions. Our study provides a comprehensive overview of remodeled proteome, which can be taken forward to elucidate the pathways that perform dual functions in stress-dependent adaptation as well as in Mtb pathogenesis.

■ ASSOCIATED CONTENT

Supporting Information

The Supporting Information is available free of charge at https://pubs.acs.org/doi/10.1021/acsomega.2c03092.

Figure S1: Whole cell protein profile of mycobacteria cultured under in vitro stress conditions, Figure S2: Validation of differentially regulated proteins, Table S1: List of DEPs in untreated and stress-treated Mtb, and Table S2: List of common proteins identified between acidic stress and diamide stress (PDF)

■ AUTHOR INFORMATION

Corresponding Author

Nisheeth Agarwal − *Laboratory of Mycobacterial Genetics, Translational Health Science and Technology Institute, NCR Biotech Science Cluster, Faridabad 121001 Haryana, India;* orcid.org/0000-0001-9203-3026; Email: nisheeth@thsti.res.in

Authors

Eira Choudhary − *Laboratory of Mycobacterial Genetics, Translational Health Science and Technology Institute, NCR Biotech Science Cluster, Faridabad 121001 Haryana, India; Symbiosis School of Biomedical Sciences, Symbiosis International (Deemed University), Pune 412115 Maharashtra, India;* Present Address: Laboratory of Molecular Virology, Regional Centre for Biotechnology, NCR Biotech Science Cluster, Faridabad 121001, Haryana, India (E.S.)

Rishabh Sharma − *Laboratory of Mycobacterial Genetics, Translational Health Science and Technology Institute, NCR Biotech Science Cluster, Faridabad 121001 Haryana, India;* Present Address: Old Dental School-Oral Health Sciences, Temple University, 3223 N. Broad Street, Philadelphia, Pennsylvania 19140, United States (R.S.)

Pramila Pal − *Laboratory of Mycobacterial Genetics, Translational Health Science and Technology Institute, NCR Biotech Science Cluster, Faridabad 121001 Haryana, India; Jawaharlal Nehru University, New Delhi 110067, India*

Complete contact information is available at: https://pubs.acs.org/10.1021/acsomega.2c03092

Author Contributions

E.C., R.S., and N.A. designed the research. E.C., R.S., P.P., and N.A. performed the experiments. E.C. and N.A. analyzed the data and wrote the paper. N.A. provided overall supervision of the study. E.C. and R.S. equally contributed to this work.

Notes

The authors declare no competing financial interest.

A complete list of the proteins identified in this article can be found online. The peptide identifications and MS/MS spectra can be obtained from the ProteomeXchange Consortium via the PRIDE partner repository with the data set identifier PXD015167.

■ ACKNOWLEDGMENTS

This work was carried out with the support of institutional core funding from the Department of Biotechnology, Govt. of India. EC is thankful to the Indian Council of Medical Research, India for providing a fellowship (TB/18/2018/ECD-I). R.S. is grateful to the Science and Engineering Research Board, India for a fellowship (PDF/2017/001194). Council of Scientific and Industrial Research, India is acknowledged for providing a Senior Research Fellowship (19/06/2016(i)EU-V) to P.P. We are thankful to Dr. Vinay Nandicoori at the National Institute of Immunology, India for providing anti-PknB and anti-GroEL1 antibodies. The Advanced Technology Platform Centre (ATPC) in the NCR Biotech Science Cluster, Faridabad is acknowledged for providing proteomics support.

■ ABBREVIATIONS

DEPs	differentially expressed proteins
FC	fold-change

https://doi.org/10.1021/acsomega.2c03092
ACS Omega 2022, 7, 26749−26766

GO gene ontology
iTRAQ isobaric tags for relative and absolute quantification
Mtb *Mycobacterium tuberculosis*
PPI protein−protein interaction
WCL whole cell lysate

REFERENCES

(1) World Health Organization. Global Tuberculosis Report; 2021. https://www.who.int/publications/i/item/9789240037021
(2) Bussi, C.; Gutierrez, M. G. Mycobacterium tuberculosis infection of host cells in space and time. *FEMS Microbiol. Rev.* **2019**, *43*, 341−361.
(3) Ribet, D.; Cossart, P. How bacterial pathogens colonize their hosts and invade deeper tissues. *Microbes Infect.* **2015**, *17*, 173−183.
(4) Lenaerts, A.; Barry, C. E.; Dartois, V. Heterogeneity in tuberculosis pathology, microenvironments and therapeutic responses. *Immunol Rev.* **2015**, *264*, 288−307.
(5) Bedard, K.; Krause, K.-H. The NOX family of ROS-generating NADPH oxidases: physiology and pathophysiology. *Physiol. Rev.* **2007**, *87*, 245−313.
(6) Nathan, C.; Shiloh, M. U. Reactive oxygen and nitrogen intermediates in the relationship between mammalian hosts and microbial pathogens. *Proc. Natl. Acad. Sci. U. S. A.* **2000**, *97*, 8841−8848.
(7) Coppola, M.; Lai, R. P.; Wilkinson, R. J.; Ottenhoff, T. H. M. The In Vivo Transcriptomic Blueprint of Mycobacterium tuberculosis in the Lung. *Front. Immunol.* **2021**, *12*, No. 763364.
(8) Liu, Y.; Tan, S.; Huang, L.; Abramovitch, R. B.; Rohde, K. H.; Zimmerman, M. D.; Chen, C.; Dartois, V.; VanderVen, B.; Russell, D. G. Immune activation of the host cell induces drug tolerance in Mycobacterium tuberculosis both in vitro and in vivo. *J. Exp. Med.* **2016**, *213*, 809−825.
(9) Piddington, D. L.; Fang, F. C.; Laessig, T.; Cooper, A. M.; Orme, I. M.; Buchmeier, N. A. Cu, Zn superoxide dismutase of Mycobacterium tuberculosis contributes to survival in activated macrophages that are generating an oxidative burst. *Infect. Immun.* **2001**, *69*, 4980−4987.
(10) Edwards, K. M.; Cynamon, M. H.; Voladri, R. K.; Hager, C. C.; DeStefano, M. S.; Tham, K. T.; Lakey, D. L.; Bochan, M. R.; Kernodle, D. S. Iron-cofactored superoxide dismutase inhibits host responses to Mycobacterium tuberculosis. *Am. J. Respir. Crit. Care Med.* **2001**, *164*, 2213−2219.
(11) Bryk, R.; Lima, C. D.; Erdjument-Bromage, H.; Tempst, P.; Nathan, C. Metabolic Enzymes of Mycobacteria Linked to Antioxidant Defense by a Thioredoxin-Like Protein. *Science* **2002**, *295*, 1073−1077.
(12) Buchmeier, N. A.; Newton, G. L.; Fahey, R. C. A Mycothiol Synthase Mutant of Mycobacterium tuberculosis Has an Altered Thiol-Disulfide Content and Limited Tolerance to Stress. *J. Bacteriol.* **2006**, *188*, 6245−6252.
(13) Vandal, O. H.; Nathan, C. F.; Ehrt, S. Acid resistance in Mycobacterium tuberculosis. *J. Bacteriol.* **2009**, *191*, 4714−4721.
(14) Molle, V.; Saint, N.; Campagna, S.; Kremer, L.; Lea, E.; Draper, P.; Molle, G. pH-dependent pore-forming activity of OmpATb from Mycobacterium tuberculosis and characterization of the channel by peptidic dissection. *Mol. Microbiol.* **2006**, *61*, 826−837.
(15) Buchmeier, N.; Blanc-Potard, A.; Ehrt, S.; Piddington, D.; Riley, L.; Groisman, E. A. A parallel intraphagosomal survival strategy shared by mycobacterium tuberculosis and Salmonella enterica. *Mol. Microbiol.* **2000**, *35*, 1375−1382.
(16) Vandal, O. H.; Pierini, L. M.; Schnappinger, D.; Nathan, C. F.; Ehrt, S. A membrane protein preserves intrabacterial pH in intraphagosomal Mycobacterium tuberculosis. *Nat. Med.* **2008**, *14*, 849−854.
(17) Mawuenyega, K. G.; Forst, C. V.; Dobos, K. M.; Belisle, J. T.; Chen, J.; Bradbury, E. M.; Bradbury, A. R.; Chen, X. Mycobacterium tuberculosis Functional Network Analysis by Global Subcellular Protein Profiling. *Mol. Biol. Cell* **2005**, *16*, 396−404.
(18) Cho, S. H.; Goodlett, D.; Franzblau, S. ICAT-based comparative proteomic analysis of non-replicating persistent Mycobacterium tuberculosis. *Tuberculosis* **2006**, *86*, 445−460.
(19) Gopinath, V.; Raghunandanan, S.; Gomez, R. L.; Jose, L.; Surendran, A.; Ramachandran, R.; Pushparajan, A. R.; Mundayoor, S.; Jaleel, A.; Kumar, R. A. Profiling the proteome of Mycobacterium tuberculosis during dormancy and reactivation. *Mol. Cell. Proteomics* **2015**, *14*, 2160−2176.
(20) Birhanu, A. G.; Gómez-Muñoz, M.; Kalayou, S.; Riaz, T.; Lutter, T.; Yimer, S. A.; Abebe, M.; Tønjum, T. Proteome Profiling of Mycobacterium tuberculosis Cells Exposed to Nitrosative Stress. *ACS Omega* **2022**, *7*, 3470−3482.
(21) Zhao, X.; Duan, X.; Dai, Y.; Zhen, J.; Guo, J.; Zhang, K.; Wang, X.; Kuang, Z.; Wang, H.; Niu, J.; Fan, L.; Xie, J. Mycobacterium Von Willebrand factor protein MSMEG_3641 is involved in biofilm formation and intracellular survival. *Future Microbiol.* **2020**, *15*, 1033−1044.
(22) Khan, M. Z.; Singha, B.; Ali, M. F.; Taunk, K.; Rapole, S.; Gourinath, S.; Nandicoori, V. K. Nandicoori VK Redox homeostasis in Mycobacterium tuberculosis is modulated by a novel actinomycete-specific transcription factor. *EMBO J.* **2021**, *40*, No. e106111.
(23) Raynaud, C.; Papavinasasundaram, K. G.; Speight, R. A.; Springer, B.; Sander, P.; Böttger, E. C.; Colston, M. J.; Draper, P. The functions of OmpATb, a pore-forming protein of Mycobacterium tuberculosis. *Mol. Microbiol.* **2002**, *46*, 191−201.
(24) Thakur, P.; Gantasala, N. P.; Choudhary, E.; Singh, N.; Abdin, M. Z.; Agarwal, N. The preprotein translocase YidC controls respiratory metabolism in Mycobacterium tuberculosis. *Sci. Rep.* **2016**, *6*, 24998.
(25) Shilov, I. V.; Seymour, S. L.; Patel, A. A.; Loboda, A.; Tang, W. H.; Keating, S. P.; Hunter, C. L.; Nuwaysir, L. M.; Schaeffer, D. A. The Paragon Algorithm, a next generation search engine that uses sequence temperature values and feature probabilities to identify peptides from tandem mass spectra. *Mol. Cell. Proteomics* **2007**, *6*, 1638−1655.
(26) Ge, S. X.; Jung, D.; Yao, R. ShinyGO: a graphical gene-set enrichment tool for animals and plants. *Bioinformatics* **2020**, *36*, 2628−2629.
(27) Szklarczyk, D.; Gable, A. L.; Lyon, D.; Junge, A.; Wyder, S.; Huerta-Cepas, J.; Simonovic, M.; Doncheva, N. T.; Morris, J. H.; Bork, P.; Jensen, L. J.; Mering, C. V. STRING v11: Protein-protein association networks with increased coverage, supporting functional discovery in genome-wide experimental datasets. *Nucleic Acids Res.* **2019**, *47*, D607−D613.
(28) Ujcikova, H.; Eckhardt, A.; Hejnova, L.; Novotny, J.; Svoboda, P. Alterations in the Proteome and Phosphoproteome Profiles of Rat Hippocampus after Six Months of Morphine Withdrawal: Comparison with the Forebrain Cortex. *Biomedicines* **2021**, *10*, 80.
(29) Olive, A. J.; Sassetti, C. M. Metabolic crosstalk between host and pathogen: sensing, adapting and competing. *Nat. Rev. Microbiol.* **2016**, *14*, 221−234.
(30) Kruh, N. A.; Troudt, J.; Izzo, A.; Prenni, J.; Dobos, K. M. Portrait of a pathogen: the Mycobacterium tuberculosis proteome in vivo. *PLoS One* **2010**, *5*, e13938−e13938.
(31) Skåne, A.; Loose, J. S. M.; Vaaje-Kolstad, G.; Askarian, F. Comparative proteomic profiling reveals specific adaption of Vibrio anguillarum to oxidative stress, iron deprivation and humoral components of innate immunity. *J. Proteomics* **2022**, *251*, No. 104412.
(32) Vázquez-Fernández, P.; López-Romero, E.; Cuéllar-Cruz, M. A comparative proteomic analysis of Candida species in response to the oxidizing agent cumene hydroperoxide. *Arch. Microbiol.* **2021**, *203*, 2219−2228.
(33) Jung, H. J.; Sorbara, M. T.; Pamer, E. G. TAM mediates adaptation of carbapenem-resistant Klebsiella pneumoniae to antimicrobial stress during host colonization and infection. *PLoS Pathog.* **2021**, *17*, No. e1009309.
(34) Yang, J.; Liu, M.; Liu, J.; Liu, B.; He, C.; Chen, Z. Proteomic Analysis of Stationary Growth Stage Adaptation and Nutritional Deficiency Response of Brucella abortus. *Front. Microbiol.* **2020**, *11*, No. 598797.

https://doi.org/10.1021/acsomega.2c03092
ACS Omega 2022, 7, 26749−26766

(35) Cook, G. M.; Berney, M.; Gebhard, S.; Heinemann, M.; Cox, R. A.; Danilchanka, O.; Niederweis, M. Physiology of Mycobacteria. *Adv. Microb. Physiol.* **2009**, *55*, No. 09.
(36) Rachman, H.; Strong, M.; Ulrichs, T.; Grode, L.; Schuchhardt, J.; Mollenkopf, H.; Kosmiadi, G. A.; Eisenberg, D.; Kaufmann, S. H. Unique transcriptome signature of Mycobacterium tuberculosis in pulmonary tuberculosis. *Infect. Immun.* **2006**, *74*, 1233−1242.
(37) Voskuil, M. I.; Bartek, I. L.; Visconti, K.; Schoolnik, G. K. The response of Mycobacterium tuberculosis to reactive oxygen and nitrogen species. *Front. Microbiol.* **2011**, *2*, 105.
(38) Rohde, K. H.; Veiga, D. F.; Caldwell, S.; Balázsi, G.; Russell, D. G. Linking the transcriptional profiles and the physiological states of Mycobacterium tuberculosis during an extended intracellular infection. *PLoS Pathog.* **2012**, *8*, No. e1002769.
(39) Fontán, P. A.; Aris, V.; Alvarez, M. E.; Ghanny, S.; Cheng, J.; Soteropoulos, P.; Trevani, A.; Pine, R.; Smith, I. Mycobacterium tuberculosis sigma factor E regulon modulates the host inflammatory response. *J. Infect. Dis.* **2008**, *198*, 877−885.
(40) Gygi, S. P.; Rochon, Y.; Franza, B. R.; Aebersold, R. Correlation between protein and mRNA abundance in yeast. *Mol. Cell. Biol.* **1999**, *19*, 1720−1730.
(41) Coulson, G. B.; Johnson, B. K.; Zheng, H.; Colvin, C. J.; Fillinger, R. J.; Haiderer, E. R.; Hammer, N. D.; Abramovitch, R. B. Targeting Mycobacterium tuberculosis Sensitivity to Thiol Stress at Acidic pH Kills the Bacterium and Potentiates Antibiotics. *Cell Chem. Biol.* **2017**, *24*, 993−1004.e4.
(42) Piddington, D. L.; Kashkouli, A.; Buchmeier, N. A. Growth of Mycobacterium tuberculosis in a Defined Medium Is Very Restricted by Acid pH and Mg 2 Levels Mycobacterium tuberculosis grows within the phagocytic vacuoles of macrophages, where it encounters a moderately acidic and possibly nutrient-restricted. *Infect. Immun.* **2000**, *68*, 4518−4522.
(43) Rohde, K. H.; Abramovitch, R. B.; Russell, D. G. Mycobacterium tuberculosis Invasion of Macrophages: Linking Bacterial Gene Expression to Environmental Cues. *Cell Host Microbe* **2007**, *2*, 352−364.
(44) Fisher, M. A.; Plikaytis, B. B.; Shinnick, T. M. Microarray analysis of the Mycobacterium tuberculosis transcriptional response to the acidic conditions found in phagosomes. *J. Bacteriol.* **2002**, *184*, 4025−4032.
(45) Puckett, S.; Trujillo, C.; Wang, Z.; Eoh, H.; Ioerger, T. R.; Krieger, I.; Sacchettini, J.; Schnappinger, D.; Rhee, K. Y.; Ehrt, S. Glyoxylate detoxification is an essential function of malate synthase required for carbon assimilation in Mycobacterium tuberculosis. *Proc. Natl. Acad. Sci. U. S. A.* **2017**, *114*, E2225−E2232.
(46) Schnappinger, D.; Ehrt, S.; Voskuil, M. I.; Liu, Y.; Mangan, J. A.; Monahan, I. M.; Dolganov, G.; Efron, B.; Butcher, P. D.; Nathan, C.; Schoolnik, G. K. Transcriptional adaptation of Mycobacterium tuberculosis within macrophages: Insights into the phagosomal environment. *J. Exp. Med.* **2003**, *198*, 693−704.
(47) Dubnau, E.; Chan, J.; Mohan, V. P.; Smith, I. Responses of Mycobacterium tuberculosis to growth in the mouse lung. *Infect. Immun.* **2005**, *73*, 3754−3757.
(48) Katiyar, A.; Singh, H.; Azad, K. K. Identification of Missing Carbon Fixation Enzymes as Potential Drug Targets in Mycobacterium Tuberculosis. *J. Integr. Bioinform.* **2018**, *15*, 1−15.
(49) Monack, D. M.; Mueller, A.; Falkow, S. Persistent bacterial infections: The interface of the pathogen and the host immune system. *Nat. Rev. Microbiol.* **2004**, *2*, 747−765.
(50) Baker, J. J.; Abramovitch, R. B. Genetic and metabolic regulation of Mycobacterium tuberculosis acid growth arrest. *Sci. Rep.* **2018**, *8*, 4168.
(51) Guan, N.; Liu, L. Microbial response to acid stress: mechanisms and applications. *Appl. Microbiol. Biotechnol.* **2020**, *104*, 51−65.
(52) Baker, J. J.; Johnson, B. K.; Abramovitch, R. B. Slow growth of Mycobacterium tuberculosis at acidic pH is regulated by phoPR and host-associated carbon sources. *Mol. Microbiol.* **2014**, *94*, 56−69.
(53) Gores, G. J.; Flarsheim, C. E.; Dawson, T. L.; Nieminen, A. L.; Herman, B.; Lemasters, J. J. Swelling, reductive stress, and cell death during chemical hypoxia in hepatocytes. *Am. J Physiol. Cell Physiol.* **1989**, *257*, C347−C354.
(54) Bruno-Bárcena, J. M.; Azcárate-Peril, M. A.; Hassan, H. M. Role of antioxidant enzymes in bacterial resistance to organic acids. *Appl. Environ. Microbiol.* **2010**, *76*, 2747−2753.
(55) Wilkins, J. C.; Homer, K. A.; Beighton, D. Analysis of Streptococcus mutans Proteins Modulated by Culture under Acidic Conditions. *Appl. Environ. Microbiol.* **2002**, *68*, 2382−2390.
(56) Kim, J.-S.; Sung, M.-H.; Kho, D.-H.; Lee, J. K. Induction of manganese-containing superoxide dismutase is required for acid tolerance in Vibrio vulnificus. *J. Bacteriol.* **2005**, *187*, 5984−5995.
(57) Mols, M.; Van Kranenburg, R.; Van Melis, C. C. J.; Moezelaar, R.; Abee, T. Analysis of acid-stressed Bacillus cereus reveals a major oxidative response and inactivation-associated radical formation. *Environ. Microbiol.* **2010**, *12*, 873−885.
(58) Hillas, P. J.; del Alba, F.; Oyarzabal, J.; Wilks, A.; Ortiz de Montellano, P. R. The AhpC and AhpD antioxidant defense system of Mycobacterium tuberculosis. *J. Biol. Chem.* **2000**, *275*, 18801−18809.
(59) Jones, C. M.; Wells, R. M.; Madduri, A. V.; Renfrow, M. B.; Ratledge, C.; Moody, D. B.; Niederweis, M. Self-poisoning of Mycobacterium tuberculosis by interrupting siderophore recycling. *Proc. Natl. Acad. Sci. U. S. A.* **2014**, *111*, 1945−1950.
(60) Gold, B.; Rodriguez, G. M.; Marras, S. A.; Pentecost, M.; Smith, I. The Mycobacterium tuberculosis ideR is a dual functional regulator that controls transcription of genes involved in iron acquisition, iron storage and survival in macrophages. *Mol. Microbiol.* **2001**, *42*, 851−865.
(61) Matthews, S. J.; Pacholarz, K. J.; France, A. P.; Jowitt, T. A.; Hay, S.; Barran, P. E.; Munro, A. W. MhuD from Mycobacterium tuberculosis: Probing a Dual Role in Heme Storage and Degradation. *ACS Infect Dis.* **2019**, *5*, 1855−1866.
(62) Levitte, S.; Adams, K. N.; Berg, R. D.; Cosma, C. L.; Urdahl, K. B.; Ramakrishnan, L. Mycobacterial Acid Tolerance Enables Phagolysosomal Survival and Establishment of Tuberculous Infection In Vivo. *Cell Host Microbe* **2016**, *20*, 250−258.
(63) Baker, J. J.; Dechow, S. J.; Abramovitch, R. B. Acid Fasting: Modulation of Mycobacterium tuberculosis Metabolism at Acidic pH. *Trends Microbiol.* **2019**, *27*, 942−953.
(64) Gonzalo Asensio, J.; Maia, C.; Ferrer, N. L.; Barilone, N.; Laval, F.; Soto, C. Y.; Winter, N.; Daffé, M.; Gicquel, B.; Martín, C.; Jackson, M. The virulence-associated two-component PhoP-PhoR system controls the biosynthesis of polyketide-derived lipids in Mycobacterium tuberculosis. *J. Biol. Chem.* **2006**, *281*, 1313−1316.
(65) Goto, Y.; Calciano, L. J.; Fink, A. L. Acid-induced folding of proteins. *Proc. Natl. Acad. Sci. U. S. A.* **1990**, *87*, 573−577.
(66) Jeong, K. C.; Hung, K. F.; Baumler, D. J.; Byrd, J. J.; Kaspar, C. W. Acid stress damage of DNA is prevented by Dps binding in Escherichia coli O157:H7. *BMC Microbiol.* **2008**, *8*, 181.
(67) Tucker, D. L.; Tucker, N.; Conway, T. Gene expression profiling of the pH response in Escherichia coli. *J. Bacteriol.* **2002**, *184*, 6551−6558.
(68) Diaz-Torres, M. L.; Russell, R. R. HtrA protease and processing of extracellular proteins of Streptococcus mutans. *FEMS Microbiol. Lett.* **2001**, *204*, 23−28.
(69) Phan-Thanh, L.; Mahouin, F. A proteomic approach to study the acid response in Listeria monocytogenes. *Electrophoresis* **1999**, *20*, 2214−2224.
(70) Martín-Galiano, A. J.; Overweg, K.; Ferrándiz, M. J.; Reuter, M.; Wells, J. M.; de la Campa, A. G. Transcriptional analysis of the acid tolerance response in Streptococcus pneumoniae. *Microbiology* **2005**, *151*, 3935−3946.
(71) Cortes, T.; Schubert, O. T.; Banaei-Esfahani, A.; Collins, B. C.; Aebersold, R.; Young, D. B. Delayed effects of transcriptional responses in Mycobacterium tuberculosis exposed to nitric oxide suggest other mechanisms involved in survival. *Sci. Rep.* **2017**, *7*, 8208.
(72) Jonas, K.; Liu, J.; Chien, P.; Laub, M. T. Proteotoxic Stress Induces a Cell-Cycle Arrest by Stimulating Lon to Degrade the Replication Initiator DnaA. *Cell* **2013**, *154*, 623−636.

https://doi.org/10.1021/acsomega.2c03092
ACS Omega 2022, 7, 26749−26766

(73) Kosower, N. S.; Kosower, E. M.; Wertheim, B.; Correa, W. S. Diamide, a new reagent for the intracellular oxidation of glutathione to the disulfide. *Biochem. Biophys. Res. Commun.* **1969**, *37*, 593−596.
(74) Mavi, P. S.; Singh, S.; Kumar, A. Reductive Stress: New Insights in Physiology and Drug Tolerance of Mycobacterium. *Antioxidants Redox Signal.* **2020**, *32*, 1348−1366.
(75) Leichert, L. I.; Scharf, C.; Hecker, M. Global characterization of disulfide stress in Bacillus subtilis. *J. Bacteriol.* **2003**, *185*, 1967−1975.
(76) Akif, M.; Khare, G.; Tyagi, A. K.; Mande, S. C.; Sardesai, A. A. Functional studies of multiple thioredoxins from Mycobacterium tuberculosis. *J. Bacteriol.* **2008**, *190*, 7087−7095.
(77) Carmel-Harel, O.; Storz, G. Roles of the Glutathione- and Thioredoxin-Dependent Reduction Systems in the Escherichia Coli and Saccharomyces Cerevisiae Responses to Oxidative Stress. *Annu. Rev. Microbiol.* **2000**, *54*, 439−461.
(78) Lin, K.; O'Brien, K. M.; Trujillo, C.; Wang, R.; Wallach, J. B.; Schnappinger, D.; Ehrt, S. Mycobacterium tuberculosis Thioredoxin Reductase Is Essential for Thiol Redox Homeostasis but Plays a Minor Role in Antioxidant Defense. *PLoS Pathog.* **2016**, *12*, No. e1005675.
(79) Stewart, G. R.; Wernisch, L.; Stabler, R.; Mangan, J. A.; Hinds, J.; Laing, K. G.; Young, D. B.; Butcher, P. D. Dissection of the heat-shock response in Mycobacterium tuberculosis using mutants and microarrays. *Microbiology* **2002**, *148*, 3129−3138.
(80) Burns, K. E.; Baumgart, S.; Dorrestein, P. C.; Zhai, H.; McLafferty, F. W.; Begley, T. P. Reconstitution of a New Cysteine Biosynthetic Pathway in Mycobacterium tuberculosis. *J. Am. Chem. Soc.* **2005**, *127*, 11602−11603.
(81) Voss, M.; Nimtz, M.; Leimkühler, S. Elucidation of the dual role of mycobacterial MoeZR in molybdenum cofactor biosynthesis and cysteine biosynthesis. *PLoS One* **2011**, *6*, No. e28170.
(82) McGillivray, A.; Golden, N. A.; Gautam, U. S.; Mehra, S.; Kaushal, D. The Mycobacterium tuberculosis Rv2745c plays an important role in responding to redox stress. *PLoS One* **2014**, *9*, No. e93604.
(83) Senaratne, R. H.; De Silva, A. D.; Williams, S. J.; Mougous, J. D.; Reader, J. R.; Zhang, T.; Chan, S.; Sidders, B.; Lee, D. H.; Chan, J.; Bertozzi, C. R.; Riley, L. W. 5′-Adenosinephosphosulphate reductase (CysH) protects Mycobacterium tuberculosis against free radicals during chronic infection phase in mice. *Mol. Microbiol.* **2006**, *59*, 1744−1753.
(84) Cambier, C. J.; Takaki, K. K.; Larson, R. P.; Hernandez, R. E.; Tobin, D. M.; Urdahl, K. B.; Cosma, C. L.; Ramakrishnan, L. Mycobacteria manipulate macrophage recruitment through coordinated use of membrane lipids. *Nature* **2014**, *505*, 218−222.
(85) Howard, N. C.; Marin, N. D.; Ahmed, M.; Rosa, B. A.; Martin, J.; Bambouskova, M.; Sergushichev, A.; Loginicheva, E.; Kurepina, N.; Rangel-Moreno, J.; Chen, L.; Kreiswirth, B. N.; Klein, R. S.; Balada-Llasat, J. M.; Torrelles, J. B.; Amarasinghe, G. K.; Mitreva, M.; Artyomov, M. N.; Hsu, F. F.; Mathema, B.; Khader, S. A. Mycobacterium tuberculosis carrying a rifampicin drug resistance mutation reprograms macrophage metabolism through cell wall lipid changes. *Nat. Microbiol.* **2018**, *3*, 1099−1108.
(86) Augenstreich, J.; Haanappel, E.; Sayes, F.; Simeone, R.; Guillet, V.; Mazeres, S.; Chalut, C.; Mourey, L.; Brosch, R.; Guilhot, C.; Astarie-Dequeker, C. Phthiocerol Dimycocerosates From Mycobacterium tuberculosis Increase the Membrane Activity of Bacterial Effectors and Host Receptors. *Front. Cell Infect. Microbiol.* **2020**, *10*, 420.
(87) Camacho, L. R.; Constant, P.; Raynaud, C.; Laneelle, M. A.; Triccas, J. A.; Gicquel, B.; Daffe, M.; Guilhot, C. Analysis of the phthiocerol dimycocerosate locus of Mycobacterium tuberculosis. Evidence that this lipid is involved in the cell wall permeability barrier. *J. Biol. Chem.* **2001**, *276*, 19845−19854.
(88) Betts, J. C.; Lukey, P. T.; Robb, L. C.; McAdam, R.; Duncan, K. Evaluation of a nutrient starvation model of Mycobacterium tuberculosis persistence by gene and protein expression profiling. *Mol. Microbiol.* **2002**, *43*, 717−731.
(89) Singh, A.; Crossman, D. K.; Mai, D.; Guidry, L.; Voskuil, M. I.; Renfrow, M. B.; Steyn, A. J. Mycobacterium tuberculosis WhiB3 Maintains redox homeostasis by regulating virulence lipid anabolism to modulate macrophage response. *PLoS Pathog.* **2009**, *5*, e1000545.
(90) Jamet, S.; Quentin, Y.; Coudray, C.; Texier, P.; Laval, F.; Daffé, M.; Fichant, G.; Cam, K. Evolution of mycolic acid biosynthesis genes and their regulation during starvation in Mycobacterium tuberculosis. *J. Bacteriol.* **2015**, *197*, 3797−3811.
(91) Torrey, H. L.; Keren, I.; Via, L. E.; Lee, J. S.; Lewis, K. High persister mutants in mycobacterium tuberculosis. *PLoS One* **2016**, *11*, e0155127.
(92) Seaver, L. C.; Imlay, J. A. Are respiratory enzymes the primary sources of intracellular hydrogen peroxide? *J. Biol. Chem.* **2004**, *279*, 48742−48750.
(93) Ehrt, S.; Schnappinger, D. Mycobacterial survival strategies in the phagosome: Defence against host stresses. *Cell. Microbiol.* **2009**, *11*, 1170−1178.
(94) Jomova, K.; Valko, M. Advances in metal-induced oxidative stress and human disease. *Toxicology* **2011**, *283*, 65−87.
(95) Sutcliffe, I. C.; Harrington, D. J. Lipoproteins of Mycobacterium tuberculosis: an abundant and functionally diverse class of cell envelope components. *FEMS Microbiol. Rev.* **2004**, *28*, 645−659.
(96) Buddelmeijer, N. The molecular mechanism of bacterial lipoprotein modification—How, when and why? *FEMS Microbiol. Rev.* **2015**, *39*, 246−261.
(97) Schmaler, M.; Jann, N. J.; Götz, F.; Landmann, R. Staphylococcal lipoproteins and their role in bacterial survival in mice. *Int. J. Med. Microbiol.* **2010**, *300*, 155−160.
(98) Reffuveille, F.; Serror, P.; Chevalier, S.; Budin-Verneuil, A.; Ladjouzi, R.; Bernay, B.; Auffray, Y.; Rincé, A. The prolipoprotein diacylglyceryl transferase (Lgt) of Enterococcus faecalis contributes to virulence. *Microbiology* **2012**, *158*, 816−825.
(99) Pathak, R.; Rathor, N.; Garima, K.; Sharma, N. K.; Singh, P.; Varma-Basil, M.; Bose, M. lspA gene of Mycobacterium tuberculosis co-transcribes with Rv1540 and induced by surface and acidic stress. *Gene* **2015**, *560*, 57−62.
(100) Su, H.; Zhu, S.; Zhu, L.; Huang, W.; Wang, H.; Zhang, Z.; Xu, Y. Recombinant lipoprotein Rv1016c derived from Mycobacterium tuberculosis is a TLR-2 ligand that induces macrophages apoptosis and inhibits MHC II antigen processing. *Front. Cell Infect. Microbiol.* **2016**, *6*, 147.
(101) Morikawa, K.; Ohniwa, R. L.; Kim, J.; Maruyama, A.; Ohta, T.; Takeyasu, K. Bacterial nucleoid dynamics: oxidative stress response in Staphylococcus aureus. *Genes Cells* **2006**, *11*, 409−423.
(102) Mangan, M. W.; Lucchini, S.; Ó Cróinín, T.; Fitzgerald, S.; Hinton, J. C. D.; Dorman, C. J. Nucleoid-associated protein HU controls three regulons that coordinate virulence, response to stress and general physiology in Salmonella enterica serovar Typhimurium. *Microbiology* **2011**, *157*, 1075−1087.
(103) Oberto, J.; Nabti, S.; Jooste, V.; Mignot, H.; Rouviere-Yaniv, J. The HU regulon is composed of genes responding to anaerobiosis, acid stress, high osmolarity and SOS induction. *PLoS One* **2009**, *4*, No. e4367.
(104) Stojkova, P.; Spidlova, P.; Lenco, J.; Rehulkova, H.; Kratka, L.; Stulik, J. HU protein is involved in intracellular growth and full virulence of Francisella tularensis. *Virulence* **2018**, *9*, 754−770.
(105) Almarza, O.; Núñez, D.; Toledo, H. The DNA-Binding Protein HU has a Regulatory Role in the Acid Stress Response Mechanism in Helicobacter pylori. *Helicobacter* **2015**, *20*, 29−40.
(106) Chawla, M.; Mishra, S.; Anand, K.; Parikh, P.; Mehta, M.; Vij, M.; Verma, T.; Singh, P.; Jakkala, K.; Verma, H. N.; AjitKumar, P.; Ganguli, M.; Narain Seshasayee, A. S.; Singh, A. Redox-dependent condensation of the mycobacterial nucleoid by WhiB4. *Redox Biol.* **2018**, *19*, 116−133.
(107) Rodríguez, J. G.; Hernández, A. C.; Helguera-Repetto, C.; Aguilar Ayala, D.; Guadarrama-Medina, R.; Anzóla, J. M.; Bustos, J. R.; Zambrano, M. M.; González-Y-Merchand, J.; García, M. J.; Del Portillo, P. Global adaptation to a lipid environment triggers the dormancy-related phenotype of Mycobacterium tuberculosis. *MBio* **2014**, *5*, No. e01125.

https://doi.org/10.1021/acsomega.2c03092
ACS Omega 2022, 7, 26749−26766

(108) Singh, V. K.; Srivastava, M.; Dasgupta, A.; Singh, M. P.; Srivastava, R.; Srivastava, B. S. Increased virulence of Mycobacterium tuberculosis H37Rv overexpressing LipY in a murine model. *Tuberculosis* **2014**, *94*, 252−261.
(109) Lee, J.-H.; Karakousis, P. C.; Bishai, W. R. Roles of SigB and SigF in the Mycobacterium tuberculosis sigma factor network. *J. Bacteriol.* **2008**, *190*, 699−707.

https://doi.org/10.1021/acsomega.2c03092
ACS Omega 2022, 7, 26749−26766